A scalar extended Higgs sector and a potential Dark Matter candidate

Hannah Tillim

Department of Physics

Royal Holloway University of London

Final project report for

PH3110: Experimental Or Theoretical Project

February 2016

Abstract

A scalar field ϕ charged under a non-SM $U(1)$ symmetry is introduced to the Higgs sector of the Lagrangian with a term mixing ϕ with the Higgs field. Both fields develop a vacuum expectation value, leading to mass mixing between the two states which is diagonalised into mass eigenstates h' (identified with the SM Higgs) and ϕ'. The Feynman rules and decay width for h' to the new particle is calculated. Fermionic fields Ψ_1 and Ψ_2, also charged under this hidden $U(1)$, are added via a Yakawa interaction with the ϕ, and their annihilation cross section to several species of SM particle calculated. Measured constraints allow the fixing of some parameters, and it is seen that with judicious choice of the remaining, the fermion's relic abundance may satisfy the requirements for Dark Matter abundance. A more granular study with fewer approximations would allow further parameterisation of the model.

Contents

List of Figures

Introduction

The purpose of this BSc project has been to investigate some of the mathematics and techniques of quantum field theory, including the nature of symmetry transformations, gauge theories and Spontaneous Symmetry Breaking (SSB), first by recreating the Standard Model (SM) Higgs SSB, and then by examining the effect of adding non-SM symmetries and fields, with a view to proposing a Dark Matter candidate.

This investigation focused first on the theoretical basis of SSB (Chapter 1), beginning with the use of a Lagrangian density to model the nature and behaviour of quantum fields, and the restrictions placed upon its form by the requirements of symmetry. This led naturally to gauge theories, and then to the Higgs mechanism and SSB. The effects of SSB on the relevant sectors of the SM Lagrangian were calculated and the manner in which the gauge bosons gain mass through the Higgs mechanism observed first-hand.

The second part of the project (Chapter 2) involved introducing a complex scalar field ϕ which was charged only under a non-SM symmetry, mixed with the Higgs field, and which also developed a vacuum expectation value. It was seen that this creates mass mixing between the two fields, and by diagonalising the system into mass eigenstates h' and ϕ', the coupling of SM particles to this new field was observed.

The next task (Chapter 3) was to suppose fermionic fields Ψ_1 and Ψ_2 (also charged under the non-SM symmetry) which enter the Lagrangian via a Yakawa interaction with ϕ. After the substitution of the mass eigenstates, the Ψs couple to the Higgs; thus, our ϕ exists as a 'portal' between non-SM and SM particles. This serves as a demonstration in miniature of the manner in which such portals have been proposed as routes to Dark Matter candidates.

Chapter 1

Theoretical background

1.1 Gauge theories

In quantum field theory, a system of fields can be described by its Lagrangian density $\mathcal{L}$ (henceforth referred to as the Lagrangian). The form of the Lagrangian depends on three qualities: renormalisability, particle content, and symmetry. The first of these was beyond the scope of this project, but pertinently it restricts the allowed dimensionality of individual terms. Particle content self-evidently depends on the phenomena one wishes to study, and governs which fields one chooses to include.

It is the final requirement of symmetry that has given rise to the need for gauge theories. When we include a particle's field in the Lagrangian, we must specify the symmetry groups under which it is 'charged' - in other words, which transformations will affect the field terms and in what way.

For example, some field P_T may be charged under an $U(1)$ symmetry transformation, meaning that it transforms (in a manner parameterised by ω) as

$$P_T \to P_T' = e^{-i\omega} P_T. \tag{1.1}$$

In contrast, a field P_U uncharged under that symmetry would transform trivially:

$$P_U \to P_U' = P_U. \tag{1.2}$$

However, while the fields within the Lagrangian may transform under various groups, the Lagrangian as a whole should not change. This is straightforward to guarantee when the transformations are global (independent of spacetime position). For instance, for the operation described in equation 1.1, one could compensate for the transformation by only including terms (such as $|P_T|^2$) where the complex conjugate cancels out the exponential after transformation.

On the other hand, local transformations (those where $\omega = \omega(x)$), cannot be accounted for in this way. For example, consider the presence of a spacetime derivative ∂_μ:

$$\mathcal{L} = \bar{\psi}\partial_\mu\psi. \tag{1.3}$$

Suppose ψ transforms under a local $U(1)$ transformation as

$$\psi \to \psi' = e^{-i\omega(x)}\psi. \tag{1.4}$$

The transformed Lagrangian is

$$\begin{aligned}
\mathcal{L}' &= \bar{\psi}'\partial_\mu\psi' \\
&= e^{i\omega(x)}\bar{\psi}\partial_\mu\left(e^{-i\omega(x)}\psi\right) \\
&= e^{i\omega(x)}\bar{\psi}\left(e^{-i\omega(x)}\partial_\mu\psi - ie^{-i\omega(x)}(\partial_\mu\omega(x))\psi\right) \\
&= \bar{\psi}\partial_\mu\psi - i\bar{\psi}(\partial_\mu\omega(x))\psi \\
&= \mathcal{L} - i\bar{\psi}(\partial_\mu\omega(x))\psi
\end{aligned} \tag{1.5}$$

The Lagrangian as it is is not invariant under this local transformation, conjuring an extra term due to the spacetime derivative. We can, however, substitute the *covariant derivative*

$$D_\mu = \partial_\mu + iqA_\mu, \tag{1.6}$$

where A_μ is a gauge field term which transforms as

$$A_\mu \to A'_\mu = A_\mu - \frac{1}{q}\partial_\mu\omega(x). \tag{1.7}$$

and q is the 'coupling constant', quantifying the strength of interaction between

ψ and A_μ.

A_μ is specified in just such a way as to cancel out the extraneous terms arising from the initial particle transformations, leaving the Lagrangian invariant:

$$\begin{aligned}
\mathcal{L}' &= \bar{\psi}' D_\mu \psi' \\
&= \bar{\psi}' \left(\partial_\mu + iqA'_\mu\right) \psi' \\
&= \bar{\psi}' \partial_\mu \psi' + \bar{\psi}' iqA'_\mu \psi' \\
&= \bar{\psi}' \partial_\mu \psi' + iqe^{i\omega(x)} \bar{\psi} (A_\mu - \frac{1}{q}\partial_\mu \omega(x)) e^{-i\omega(x)} \psi' \\
&= \bar{\psi}\partial_\mu \psi - i\bar{\psi}(\partial_\mu \omega(x))\psi + iq\bar{\psi}A_\mu \psi - i\bar{\psi}(\partial_\mu \omega(x))\psi \\
&= \bar{\psi}\left(\partial_\mu + iqA_\mu\right)\psi \\
&= \bar{\psi} D_\mu \psi
\end{aligned} \tag{1.8}$$

After gauging the field, we also observe terms that indicate the existence of new particles: the gauge bosons. There will be different forms of gauge fields to compensate for different types of transformations under which the fields transform. The Standard Model Lagrangian is gauge invariant under $SU(2)_L \times U(1)_Y \times SU(3)_c$, which requires the appearance of the the $W^\pm$ and Z bosons and the photon (see section 1.2) from $SU(2)_L \times U(1)_Y$ as well as 8 gluons from $SU(3)_c$.

We must add in for each boson A_μ a kinetic term,

$$F_{\mu\nu} = \partial_\mu A_\nu - \partial_\nu A_\mu. \tag{1.9}$$

This term is gauge invariant, but not Lorentz invariant. Thus the final addition must be a Lorentz scalar of the form $F_{\mu\nu}F^{\mu\nu}$.

1.2 Spontaneous symmetry breaking

The gauging of the SM to compensate for transformations under the group $SU(2)_L \times U(1)_Y$ initially predicted massless gauge bosons. However, experiments measured large masses for both - 80.4 GeV for $W^\pm$ and 91.2 GeV for Z. To add a mass term by hand would explicitly break the symmetry of the Lagrangian. The solution, proposed by several groups in the 1960s, involves the existence of a field which transforms under the same symmetry and has a non-zero minimum potential value - a vacuum expectation value (vev) - upon which the masses of the bosons depend. The existence of a vev which does not respect a symmetry is known as spontaneous symmetry breaking, to contrast with explicit symmetry breaking.

The relevant part of the SM Lagrangian is

$$\mathcal{L}_{EW} = -\frac{1}{4}F^a_{\mu\nu}F^{a\mu\nu} - \frac{1}{4}G_{\mu\nu}G^{\mu\nu} + |\mathbf{D}_\mu H|^2 - V(H), \tag{1.10}$$

where the kinetic terms for the gauge fields B_μ and W_μ are

$$F^a_{\mu\nu} = \partial_\mu W^a_\nu - \partial_\nu W^a_\mu - g f^{abc} W^b_\mu W^c_\nu \tag{1.11}$$

and

$$G_{\mu\nu} = \partial_\mu B_\nu - \partial_\nu B_\mu, \tag{1.12}$$

the covariant derivative of the 'Higgs' field H is

$$\mathbf{D}_\mu = \partial_\mu + \frac{ig'}{2}B_\mu + \frac{ig}{2}\tau^i W^i_\mu, \qquad (i = 1, 2, 3) \tag{1.13}$$

with τ^i representing the Pauli matrices, and the potential is given by

$$V(H) = -\mu^2 H_i^\dagger H^i + \lambda(H_i^\dagger H^i)^2. \tag{1.14}$$

B_μ and W_μ are the gauge fields associated with local $U(1)_Y$ and $SU(2)_L$ symmetries respectively and the Higgs is a complex doublet with coupling constants g and g' with the gauge fields.

The negative sign before μ creates the famous 'Mexican hat' potential, with a non-zero minimum value. Solving for the minimum with respect to H, we find

$$\langle H \rangle = e^{i\theta} \begin{pmatrix} 0 \\ \frac{\mu}{\sqrt{2\lambda}} \end{pmatrix}. \tag{1.15}$$

There are thus an infinite number of degenerate vacuua distinguished by their phase. Visually, these lie along the valley of the potential in Figure 1.1. The choice of phase breaks the symmetry spontaneously. We choose $\theta = 0$ to obtain

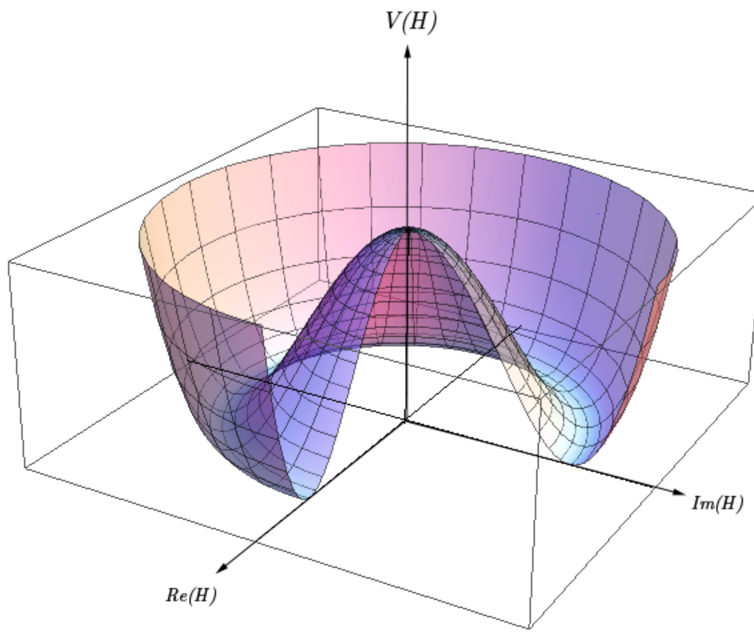

Figure 1.1: The 'Mexican hat' potential of the Higgs field.

the vev

$$v = \sqrt{\frac{\mu^2}{\lambda}}, \tag{1.16}$$

And expand the Higgs doublet around this value:

$$H = \begin{pmatrix} g_1 \\ \frac{1}{\sqrt{2}}(v + h + ig_0) \end{pmatrix}. \tag{1.17}$$

In the unitary gauge, the g_0 and g_1 terms (the Goldstone bosons) can be gauged away to zero. We insert this doublet into 1.10, and substitute:

$$\begin{aligned} W_\mu^\pm &= \frac{W_\mu^1 \mp W_\mu^2}{\sqrt{2}}, \\ W_\mu^0 &= W_\mu^3, \end{aligned} \tag{1.18}$$

so that

$$|\mathbf{D}_\mu H|^2 = \frac{1}{2}(\partial_\mu h)^2 + \frac{g^2 v^2}{4} W^{+\mu} W^-_\mu + \frac{v^2}{8}(gW^0_\mu - g' B_\mu)^2 \\ + \frac{g^2}{4} W^{+\mu} W^-_\mu (2vh + h^2) + \frac{1}{8}(gW^0_\mu - g' B_\mu)^2 (2vh + h^2). \tag{1.19}$$

We find mass terms for $W^\pm, W^0$ and B, and also a mass term in $W^0_\mu B_\mu$. This is an example of mass mixing. The W^0 and B fields are linear combinations of the 'mass eigenstate' fields A_μ and Z_μ (identified with the photon and Z boson respectively):

$$\begin{pmatrix} Z \\ A \end{pmatrix} = \begin{pmatrix} \cos\theta_W & -\sin\theta_W \\ \sin\theta_W & \cos\theta_W \end{pmatrix} \begin{pmatrix} W^0 \\ B^0 \end{pmatrix}, \tag{1.20}$$

were θ_W is the Weinberg angle.

By inserting the correct linear combinations, the system is diagonalised i.e. it is expressed in terms of A_μ and Z_μ, which have no mass mixing: they are the observable mass eigenstates. The Lagrangian becomes:

$$\begin{aligned} \mathcal{L}_{EW} = &+\frac{1}{2}\left((\partial_\mu h)^2 - \mu^2 h^2)\right) \\ &- \frac{1}{4}(\partial_\mu W^+_\nu - \partial_\nu W^+_\mu)(\partial^\mu W^{+\nu} - \partial^\nu W^{+\mu}) + \frac{1}{8} g^2 v^2 W^{+2} \\ &- \frac{1}{4}(\partial_\mu W^-_\nu - \partial_\nu W^-_\mu)(\partial^\mu W^{-\nu} - \partial^\nu W^{-\mu}) + \frac{1}{8} g^2 v^2 W^{-2} \\ &- \frac{1}{4}(\partial_\mu Z_\nu - \partial_\nu Z_\mu)(\partial^\mu Z^\nu - \partial^\nu Z^\mu) + \frac{1}{8}(g^2 + g'^2)^2 v^2 Z^2 \\ &- \frac{1}{4}(\partial_\mu A_\nu - \partial_\nu A_\mu)(\partial^\mu A^\nu - \partial^\nu A^\mu). \end{aligned} \tag{1.21}$$

The boson masses are:

$$\begin{aligned} M_{W^\pm} &= \frac{gv}{2} \\ M_Z &= \frac{v}{2}(g^2 + g'^2)^{1/2} \\ M_\gamma &= \frac{1}{2}\left(g_1^2 + g_2^2\right)\sin^2\theta_W \quad = 0 \end{aligned} \tag{1.22}$$

from which it is quite clear the weak boson masses arise from the non-zero value of the Higgs vev and that the photon is massless due to the choice of the unitary gauge. The degrees of freedom belonging to the Higgs (the Goldstone bosons) are eaten by the electroweak bosons' longitudinal components, giving them a mass degree of freedom.

1.3 Yukawa interactions

SM fermions also lack masses before the Higgs develops a vev. They gain the mass during SSB due to their involvement in a *Yakawa* interaction; a term of the Lagrangian that mixes left-handed doublet and right-handed singlet fermions with the Higgs field.

$$\mathcal{L}_{Yakawa} = -\lambda_f \bar{f_L}^i H_i f_R + h.c. \tag{1.23}$$

such that the entire term has zero net charge under all symmetries. For example, for the case of hypercharge Y in the Yakawa interaction between leptons and the Higgs scalar:

$$\begin{aligned} Y(\bar{l_L}^i) &= \frac{1}{2}, \\ Y(e_R) &= -1, \\ Y(H) &= \frac{1}{2}, \end{aligned} \tag{1.24}$$

and therefore

$$Y_{tot} = -1 + \frac{1}{2} + \frac{1}{2} = 0. \tag{1.25}$$

When the Higgs is expanded about its vev, the fermion picks up a mass term dependent on that vev.

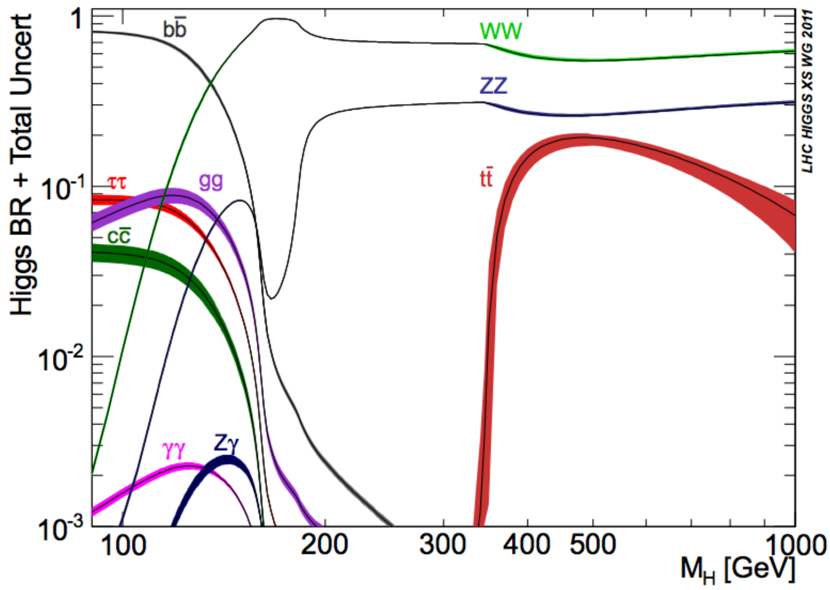

Figure 1.2: Decays of the SM Higgs to SM particles (taken from [12]).

1.4 Higgs decay and invisible states

The Higgs decays into other SM particles either directly or via loops, with decay rates predicted by the theory dependent on the Higgs mass m_h (see Figure 1.2). Higgs searches at the LHC measured a signal at 125 GeV in 2012, now positively identified as the Higgs [5].

The decay rate of a particle to its products is usually calculated by constructing a Feynman diagram of the decay; the factor associated with the vertex is the coefficient of the relevant term in the Lagrangian. The Higgs couples to all massive SM particles and interacts with any particle with which it shares a suitable Lagrangian term.

In this report, we will discuss the possibility of Higgs interaction with non-SM 'hidden' states. It has been calculated in [1] that the branching ratio to 'invisible' states of the Higgs with SM couplings but additional decay modes is:

$$\mathcal{B}_{invis} < 0.23. \tag{1.26}$$

1.4.1 Higgs portals

Along with the fields charged under the SM symmetry $SU(2)_L \times U(1)_Y \times SU(3)_c$, there is no reason not to suppose the existence of fields charged under non-SM symmetries, which may be added to the SM Lagrangian as a 'hidden sector'. If, in addition, a term is added to the Higgs sector potential (1.14) which mixes a new scalar field ϕ with H, one can couple SM particles to further hidden fields through the mass mixing between the boson of the H field and that of the hidden scalar field (see [10] for a brief overview).

One procedure (explored in [13] and [3]) is to suppose the existence of a complex scalar field ϕ which is charged under a non-SM $U(1)$ symmetry, $U(1)_D$ but is a singlet under the SM gauge symmetries. We have employed this approach in this project, introducing mixing between ϕ and the Higgs field and showing how this leads to the coupling of the diagonalised mass state ϕ' and the SM particles. We then propose two fermionic fields Ψ_1 and Ψ_2, which interact with ϕ via a Yakawa term, and observe that this leads to coupling of the Ψs to h' and ϕ', and, through that 'portal', to the SM particles.

Other approaches include using different forms of the hidden fields and their couplings in the potential (e.g. [7]), or requiring symmetry under different transformations such as Z_2 [6].

1.4.2 Calculating cross sections and decays

It will at some stage of the report be necessary for us to derive the decay widths Γ and interaction cross sections σ for various processes in order to compare our model with observations. This involves first calculating the *matrix element* $\mathcal{M}$ for each interaction, and then integrating over the phase space of the final states.

For the interaction $1+2 \to 3+4$, the interaction cross section is given by [11]:

$$d\sigma = \frac{1}{v_{rel}} \frac{1}{2p_1^0} \frac{1}{2p_2^0} |\mathcal{M}|^2 (2\pi)^4 \delta^{(4)}(p_1 + p_2 - p_3 - p_4) \frac{d^3p_3}{(2\pi)^3} \frac{1}{2p_3^0} \frac{d^3p_4}{(2\pi)^3} \frac{1}{2p_4^0}, \qquad (1.27)$$

where v_{rel} is the relative velocity between 1 and 2.

For a particle A decaying to final states f with momenta p_f, the decay width is given by [11]:

$$d\Gamma = \frac{1}{2m_A} \prod_f \left(\frac{d^3p}{(2\pi)^3} \frac{1}{2p_f^0} \right) |\mathcal{M}(m_A \to p_f)|^2 (2\pi)^4 \delta^{(4)}(p_A - \sum p_f). \tag{1.28}$$

For a two-particle final state, this simplifies to

$$\Gamma = \frac{1}{2m_A} \int \frac{d^3p}{(2\pi)^3} \frac{1}{2p^0} \frac{d^3k}{(2\pi)^3} \frac{1}{2k^0} |\mathcal{M}(p,k)|^2 \, \delta^{(4)}(q - (p+k)). \tag{1.29}$$

The phase-space integrals in both cases are carried out over all possible final states of those particles. This means, in the case of identical final particles, that the integral overestimates the cross section by a factor of 2, by double counting identical arrangements. This is accounted for by dividing such cross sections by a symmetry factor $S = 2$, as will be seen in Chapter 3 in the derivations of the phase space of identical final states (those of $\phi'\phi', h'h'$ and ZZ).

1.5 Dark Matter

In Chapter 3 we will propose that our hidden fermionic field may serve as a candidate for Dark Matter. It must therefore fulfil several broad criteria on first inspection: it must be non-luminous, uncharged under electromagnetism, and be stable or extremely long-lived; the interaction between DM and SM particles must be very weak [9].

1.5.1 DM freeze-out

One can suppose that at early times, dark matter was in thermal equilibrium with the rest of the universe, and the rate of production was equal to that of annihilation. At some point, the expansion of the universe overtakes the interaction rate and the Dark Matter is decoupled from the cosmic plasma. After this, the number density per comoving volume is frozen out at a relic density, no longer suppressed by the equilibrium exponential factor [9], [8] - see Figure 1.3.

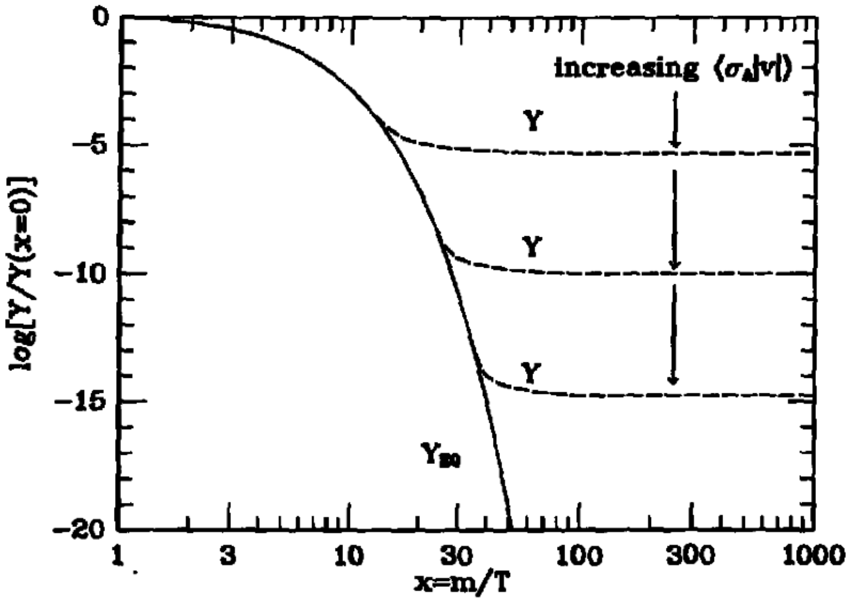

Figure 1.3: Abundance of a massive particle at thermal equilibrium (solid line) and after freeze-out (dashed lines) (taken from [8]).

We will assume in our calculations that the freeze-out temperature is below the mass of the DM - i.e., freeze-out occurs after the DM particles have become non-relativistic.

Following the argument in [8], we can expect the thermal average of the annihilation cross section multiplied by the relative velocity $\langle \sigma v \rangle$ to go as T^n, depending on the angular momentum quantum number of the interaction. We can therefore expand in terms of $\langle v^2 \rangle \propto T$ [2]:

$$\begin{aligned} \langle \sigma v \rangle &= a + b\langle v^2 \rangle + \mathcal{O}(v^4) \\ &\approx a + \frac{6b}{x}, \end{aligned} \tag{1.30}$$

where $x = \langle v^2 \rangle^{-1} = m/T$.

If $a \neq 0$, the annihilation is dominated by s-wave ($l = 0$) interactions. Otherwise, the second term on the RHS, representing p-wave ($l = 1$) interactions, dominates. The physical significance of this relates to the conservation of total angular momentum in the interaction. We anticipate that for our fermionic species (each spin 1/2) going to other states via a scalar (spin 0), all interactions will necessarily be p-wave.

We can express the dominant term as:

$$\langle \sigma v \rangle \approx \sigma_0 x^{-n}, \tag{1.31}$$

where $n = 0$ if $a \neq 0$, and $n = 1$ if $a = 0, b \neq 0$.

The relic abundance Y_∞ of DM can be found by solving the Boltzmann equation, arriving at [8]:

$$Y_\infty = \frac{3.97(n+1)x_f}{(g_{*S}/\sqrt{g_*})m_\Psi m_{Pl}\langle \sigma v \rangle} = \frac{3.97(n+1)x_f^{n+1}}{(g_{*S}/\sqrt{g_*})m_\Psi m_{Pl}\sigma_0}, \tag{1.32}$$

and an expression for the mass density:

$$\Omega_\Psi h^2 = 2.82 \times 10^8 m_\Psi Y_\infty \quad \text{GeV}^{-1}. \tag{1.33}$$

g_* is the effective number of relativistic degrees of freedom and g_{*S} the effective number of relativistic degrees of freedom for entropy:

$$\begin{aligned} g_* &= \sum_{i=\text{bosons}} g_i \left(\frac{T_i}{T}\right)^4 + \frac{7}{8} \sum_{j=\text{fermions}} g_j \left(\frac{T_i}{T}\right)^4, \\ g_{*S} &= \sum_{i=\text{bosons}} g_i \left(\frac{T_i}{T}\right)^3 + \frac{7}{8} \sum_{j=\text{fermions}} g_j \left(\frac{T_i}{T}\right)^3, \end{aligned} \tag{1.34}$$

where T is the temperature of the thermal bath, and T_i that of the individual species. These temperatures would naturally be equal when the species is in thermal equilibrium.

By comparing this with the observed value of $\Omega_\Psi h^2 = 0.11$ [8], we can evaluate the validity of our model for DM.

Chapter 2

The complex scalar field ϕ

2.1 Extending the potential

Our new particle ϕ is a complex scalar, charged under a non-SM $U(1)_D$ symmetry. Mixing between ϕ and the Higgs is introduced into our modified potential:

$$V(H,\phi) = -\mu_H|H|^2 + \lambda_H|H|^4 - \mu_\phi|\phi|^2 + \lambda_\phi|\phi|^4 + \lambda_3|H|^2|\phi|^2. \tag{2.1}$$

Due to the negative signs before μ_H and μ_ϕ, both H and ϕ develop vacuum expectation values. Differentiating to find the minimum gives us:

$$\begin{aligned} v_h &= \sqrt{\frac{2\lambda_3\mu_\phi^2 - 4\lambda_\phi\mu_H^2}{\lambda_3^2 - 4_H\lambda_\phi}} \\ v_\phi &= \sqrt{\frac{2\lambda_3\mu_H^2 - 4\lambda_H\mu_\phi^2}{\lambda_3^2 - 4_H\lambda_\phi}}. \end{aligned} \tag{2.2}$$

We expand both of our fields about their vevs:

$$\begin{aligned} H &= \begin{pmatrix} g_1 \\ \frac{1}{\sqrt{2}}(v_h + h + ig_0) \end{pmatrix} \qquad \text{and} \\ \phi &= \frac{1}{\sqrt{2}}(v_\phi + \phi_r + i\phi_i). \end{aligned} \tag{2.3}$$

where h will be identified with the SM Higgs and g_0 and g_1 represent the Goldstone bosons.

Substituting these back into the potential, we find that g_0, g_1 and ϕ_i are massless, as expected, and that there has emerged a mass term which mixes h and ϕ_r,

$$\lambda_3 v_H v_\phi h\phi_r. \tag{2.4}$$

Here we will choose the unitary gauge, in which g_0, g_1 and ϕ_i are set to zero, rendering the full potential

$$\begin{aligned} V_U(h,\phi) = {} & [\frac{1}{4}v_H\lambda 3 - \frac{1}{2}\mu_H^2 + \frac{3}{2}v_H^2\lambda_H]h^2 + [\frac{1}{2}v_H v_\phi^2\lambda_3 + v_H^3\lambda_H - v_H\mu_H^2]h + \frac{1}{4}\lambda_H h^4 \\ & + v_H\lambda_H h^3 + \frac{1}{2}v_\phi\lambda_3 h^2\phi_r + v_H v_\phi\lambda_3 h\phi_r + \frac{1}{4}\lambda_3 h^2\phi_r^2 + \frac{1}{2}v_H\lambda_3 h\phi_r^2 \\ & + [\frac{1}{2}v_H^2 v_\phi\lambda_3 + v_\phi^3\lambda_{phi} - v_\phi\mu_\phi^2]\phi_r + [\frac{1}{4}v_H^2\lambda 3 + \frac{3}{2}v_\phi^3\lambda_\phi - \frac{1}{2}\mu_\phi^2]\phi_r^2 + v_\phi\lambda_\phi\phi_r^3 \\ & + \frac{1}{4}\lambda\phi\phi_r^4 + \frac{1}{4}v_H^2 v_\phi^2\lambda_3 + \frac{1}{4}v_H^4\lambda_H + \frac{1}{4}v_\phi^4\lambda_\phi - \frac{1}{2}v_H^2\mu_H^2 - \frac{1}{2}v_\phi^2\mu_\phi^2. \end{aligned} \tag{2.5}$$

2.2 Diagonalising the mass matrix

Such mass mixing as occurs between h and ϕ_r means that these fields do not represent the observable mass eigenstates. The system must be diagonalised, as was the case for the B_μ and W_μ^0 bosons in section (1.2). We must derive the mixing angle between h and ϕ_r and our mass eigenstates, which we shall call h' and ϕ'.

$$\begin{pmatrix} h \\ \phi_r \end{pmatrix} = \begin{pmatrix} \cos\theta & -\sin\theta \\ \sin\theta & \cos\theta \end{pmatrix} \begin{pmatrix} h' \\ \phi' \end{pmatrix} \tag{2.6}$$

We obtain the mixing matrix elements from the coefficients of the h^2, ϕ_r^2 and $h\phi_r$ terms, i.e.:

$$\begin{aligned} \mathcal{L}_{h\phi mix} &= m_{11}h^2 + m_{22}\phi_r^2 + (m_{12}+m_{21})h\phi_r \\ &= \begin{pmatrix} h & \phi_r \end{pmatrix} \begin{pmatrix} m_{11} & m_{12} \\ m_{21} & m_{22} \end{pmatrix} \begin{pmatrix} h \\ \phi_r \end{pmatrix} \end{aligned} \tag{2.7}$$

where

$$m_{11} = \frac{1}{4}\left(v_\phi^2\lambda_3 + 6v_h^2\lambda_h - 2\mu_h^2\right)$$
$$m_{22} = \frac{1}{4}\left(v_h^2\lambda_3 + 6v_\phi^2\lambda_\phi - 2\mu_\phi^2\right) \tag{2.8}$$
$$m_{12} = m_{21} = \frac{1}{2}v_h v_\phi \lambda_3$$

We therefore require:

$$\begin{aligned}\begin{pmatrix} h & \phi_r \end{pmatrix}\begin{pmatrix} m_{11} & m_{12} \\ m_{21} & m_{22}\end{pmatrix}\begin{pmatrix} h \\ \phi_r \end{pmatrix} &= \begin{pmatrix} h' & \phi' \end{pmatrix}\begin{pmatrix} \cos\theta & \sin\theta \\ -\sin\theta & \cos\theta \end{pmatrix}\begin{pmatrix} m_{11} & m_{12} \\ m_{21} & m_{22}\end{pmatrix}\begin{pmatrix} \cos\theta & -\sin\theta \\ \sin\theta & \cos\theta \end{pmatrix}\begin{pmatrix} h' \\ \phi' \end{pmatrix} \\ &= \begin{pmatrix} h' & \phi' \end{pmatrix}\begin{pmatrix} m_h^2 & 0 \\ 0 & m_\phi^2 \end{pmatrix}\begin{pmatrix} h' \\ \phi' \end{pmatrix} \\ &= m_h^2 h'^2 + m_\phi^2 \phi'^2,\end{aligned} \tag{2.9}$$

where m_h and m_ϕ are clearly identified with the masses of h' and ϕ'.

We can calculate θ by multiplying out the matrices, equating one of the off-diagonal elements to zero, and using the fact that $m_{12} = m_{21}$:

$$\begin{aligned} 0 &= -m_{11}\sin\theta\cos\theta - m_{12}\sin^2\theta + m_{21}\cos^2\theta + m_{22}\sin\theta\cos\theta \\ &= m_{12}(\cos^2\theta - \sin^2\theta) + (m_{22} - m_{11})\sin\theta\cos\theta \\ &= m_{12}\cos 2\theta + \frac{m_{22} - m_{11}}{2}\sin 2\theta \\ \implies \tan 2\theta &= \frac{2m_{12}}{m_{11} - m_{22}} \end{aligned} \tag{2.10}$$

The full expression of θ in terms of $\lambda_h, \lambda_\phi, \lambda_3, \mu_h$ and μ_ϕ is given in Appendix A.

If we express h and ϕ_r as linear combinations of h' and ϕ':

$$\begin{aligned} h &= h'\cos\theta - \phi'\sin\theta \\ \phi_r &= h'\sin\theta + \phi'\cos\theta \end{aligned} \tag{2.11}$$

and substitute these into (2.5) we find that there is no coupling between the mass eigenstates, as expected.

$$V_U(h', \phi') = \frac{1}{4}\Big[\lambda_3 \left(\cos\theta h' + v_h - \sin\theta\phi'\right)^2 \left(\sin\theta h' + \cos\theta\phi' + v_\phi\right)^2 \\ + \lambda_h \left(\cos\theta h' + v_h - \sin\theta\phi'\right)^4 - 2\mu_h^2 \left(\cos\theta h' + v_h - \sin\theta\phi'\right)^2 \\ + \lambda_\phi \left(\sin\theta h' + \cos\theta\phi' + v_\phi\right)^4 - 2\mu_\phi^2 \left(\sin\theta h' + \cos\theta\phi' + v_\phi\right)^2\Big]. \tag{2.12}$$

The expanded expression of $V(h', \phi')$ is given in Appendix B.

2.3 The electroweak sector

We turn next to the electroweak kinetic sector of the SM Lagrangian, (1.10), reproduced here:

$$\mathcal{L}_{EW} = -\frac{1}{4}F^a_{\mu\nu}F^{a\mu\nu} - \frac{1}{4}G_{\mu\nu}G^{\mu\nu} + |\mathbf{D}_\mu H|^2. \tag{2.13}$$

where the terms are defined as in section 1.2.

Following the same procedure as before, we diagonalise the B_μ-Z_μ system and substitute of the Higgs expanded around its new vev. The Lagrangian now contains the usual mass terms for the electroweak bosons.

$$M_W = \frac{gv_h}{2}, \\ M_Z = \frac{gv_h}{2}\frac{1}{\cos\theta_W}. \tag{2.14}$$

We also naturally find couplings C between ϕ' or h' and the massive gauge bosons, but not the photon, which are simply the SM couplings (1.21) modulated by $\sin\theta$ or $\cos\theta$.

$$C(h'W^\pm W^\mp) = \frac{g^2 v_h}{2}\cos\theta \\ C(\phi'W^\pm W^\mp) = \frac{g^2 v_h}{2}\sin\theta \tag{2.15}$$

2.4 The hidden $U(1)_D$ sector

Finally, we include the sector involving our proposed non-SM $U(1)_D$ group, and we require that ϕ transforms under local $U(1)_D$ transformations, so that our gauged $U(1)_D$ sector reads

$$\mathcal{L}_D = -\frac{1}{4}K_{\mu\nu}K^{\mu\nu} + |D_\mu\phi|^2, \tag{2.16}$$

where $K_{\mu\nu}$ is the kinetic term for the $U(1)_D$ boson Z'_μ and ϕ has the covariant derivative with coupling constant g_D:

$$D_\mu = \partial_\mu + ig_D Z'_\mu. \tag{2.17}$$

After SSB arising from the form of the potential in 2.1, we replace ϕ with the expansion around its vev (2.3):

$$\begin{aligned}\mathcal{L}_D = &\frac{1}{2}\left(\partial_\mu\phi_r\right)^2 + \frac{1}{2}\left(\partial_\mu\phi_i\right)^2 + \frac{1}{2}g_D^2 Z'_\mu Z'^\mu\left(\phi_r^2 + \phi_i^2\right)\\ &- g_D Z'^\mu\left(\phi_i\partial_\mu\phi_r - \phi_r\partial_\mu\phi_i\right) + g_D v_\phi Z'^\mu\partial_\mu\phi_i + g_D^2 v_\phi Z'^\mu Z'_\mu\phi_r\\ &+ \frac{1}{2}g_D^2 v_\phi^2 Z'_\mu Z'^\mu.\end{aligned} \tag{2.18}$$

The final term gives a mass to Z'_μ:

$$m_{Z'} = g_D v_\phi. \tag{2.19}$$

After substituting in the value of the vev (2.2) and choosing the unitary gauge ($\phi_i = 0$), we find:

$$\begin{aligned}\mathcal{L}_D = g_D^2 Z'^2 \frac{\lambda_3\mu_h^2 - 2\lambda_h\mu_\phi}{\lambda_3^2 - 4\lambda_h\lambda_\phi} + g_D^2 \sin\theta Z'^2 h' \sqrt{\frac{2\lambda_3\mu_h^2 - 4\lambda_h\mu_\phi^2}{\lambda_3^2 - 4\lambda_h\lambda_\phi}} \\ + g_D^2 \cos\theta Z'^2 \phi' \sqrt{\frac{2\lambda_3\mu_h^2 - 4\lambda_h\mu_\phi^2}{\lambda_3^2 - 4\lambda_h\lambda_\phi}} + \frac{1}{2} g_D^2 \sin^2\theta Z'^2 h'^2 \\ + \frac{1}{2} g_D^2 \sin 2\theta Z'^2 h'\phi' + \frac{1}{2} g_D^2 \cos^2\theta Z'^2 \phi'^2 \\ + \frac{1}{2}\sin^2\theta \left(\partial_\mu h'\right)^2 + \frac{1}{2}\sin 2\theta \partial_\mu h' \partial^\mu \phi' + \frac{1}{2}\cos^2\theta \left(\partial_\mu \phi'\right)^2 .\end{aligned} \tag{2.20}$$

Z'_μ couples to h' and ϕ' in the expected way in terms dependent on g_D. However, we have chosen to assume here that the $g_D \ll 1$, neglecting discussion of Z'_μ hereafter:

$$\mathcal{L}_D \approx \frac{1}{2}\sin^2\theta \left(\partial_\mu h'\right)^2 + \frac{1}{2}\sin 2\theta \partial_\mu h' \partial^\mu \phi' + \frac{1}{2}\cos^2\theta \left(\partial_\mu \phi'\right)^2 . \tag{2.21}$$

2.5 Decay width $\Gamma(h' \to \phi'\phi')$

Our Lagrangian so far is the combination of 2.13, 2.21 and 2.12:

$$\mathcal{L} = \mathcal{L}_{EW} + \mathcal{L}_D - V(h', \phi'). \tag{2.22}$$

From this we can derive the Feynman rules for the theory. There are many diagrams in our full Lagrangian; we focus in particular on matrix element for the interaction of h' with $\phi'\phi'$ - this represents the Feynman diagram (2.1).

We can extract the matrix element (which is comprised purely of the vertex factor) in terms of θ:

$$\begin{aligned}\mathcal{M}(h' \to \phi'\phi') =& \frac{1}{4}\cos\theta v_h \left[(3\cos 2\theta - 1)\lambda_3 + 12\sin^2\theta\lambda_h\right] \\ & - \frac{1}{4}\sin\theta v_\phi \left[(3\cos 2\theta + 1)\lambda_3 - 12\sin^2\theta\lambda_\phi\right]\end{aligned} \tag{2.23}$$

The remaining vertex factors between h' and ϕ' are given in Appendix C.

In the case of the decay of h' to identical ϕ' states, $\mathcal{M}$ is independent of

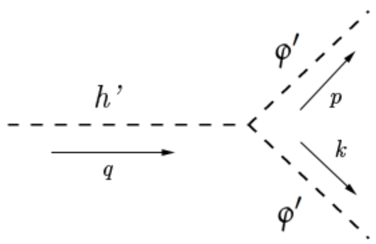

Figure 2.1: Decay of h' to $\phi'\phi'$

momenta, consisting as it does purely of the vertex factor, and we can simplify as follows [11]:

$$\Gamma = \frac{1}{2m_h} |\mathcal{M}|^2 \frac{1}{8\pi} \frac{|\mathbf{p}|}{E_{cm}} \tag{2.24}$$

where $|\mathbf{p}|$ is the momentum of the final particles in the centre-of-mass frame (i.e. the Higgs' rest frame), $E_{cm} = m_h$ and we have divided by the symmetry factor $S = 2$.

In the rest frame of the Higgs (where the momenta are as shown in Figure 2.1),

$$\begin{aligned} q^0 &= m_h \\ \mathbf{q} &= 0 \\ \mathbf{p} &= -\mathbf{k} \\ p^0 = k^0 &= \sqrt{m_\phi^2 + |\mathbf{p}|^2} \\ p.k &= \frac{m_h^2 - 2m_\phi^2}{2} \end{aligned}$$

and

$$|\mathbf{p}| = \sqrt{\frac{m_h^2}{4} - m_\phi^2} \tag{2.25}$$

Thus:

$$\Gamma = \frac{1}{4m_h}\frac{1}{128\pi}[\cos\theta v_h\left((3\cos 2\theta - 1)\lambda_3 + 12\sin^2\theta\lambda_h\right)$$
$$- \frac{1}{4}\sin\theta v_\phi\left((3\cos 2\theta + 1)\lambda_3 - 12\sin^2\theta\lambda_\phi\right)]^2\sqrt{1 - \frac{4m_\phi^2}{m_h^2}} \tag{2.26}$$

We now have the decay width in terms of our 5 parameters $\mu_H, \mu_\phi, \lambda_H, \lambda_\phi$ and λ_3, and also of m_ϕ. Our next task must be to fix some of these parameters to give a meaningful decay width as a function of those remaining.

2.5.1 Fixing the parameters

We identify h' with the SM Higgs and so:

$$\begin{aligned} m_h &= 125 \text{ GeV} \\ v_H &= 246 \text{ GeV} \end{aligned} \tag{2.27}$$

We consider the case where h' decays to two ϕ's. For this decay to be kinematically permitted, we must require that $m_\phi \leq \frac{m_h}{2}$. For the sake of argument, we choose:

$$m_\phi = 20 \text{ GeV}. \tag{2.28}$$

This allows us to solve for 3 parameters in terms of λ_3 and λ_ϕ. We further require that our h' couples to the W boson (see 2.15) with a magnitude that is within error of the measured value for SM Higgs-W coupling. Considering the uncertainties set out in [4], we will require the coupling to be within 10% of the observed value.

$$\begin{aligned} \frac{g^2 v_h}{2}\cos\theta &\geq 0.9\frac{g^2 v_h}{2} \\ \therefore \cos\theta &\geq 0.9 \end{aligned} \tag{2.29}$$

In Figure 2.2, values of λ_3 and λ_ϕ which fulfil the requirement in (2.29) are filled in.

Both λ_3 and λ_ϕ must be appreciably smaller than 4π to allow for perturbative expansions. This can be schematically justified by examining the series of

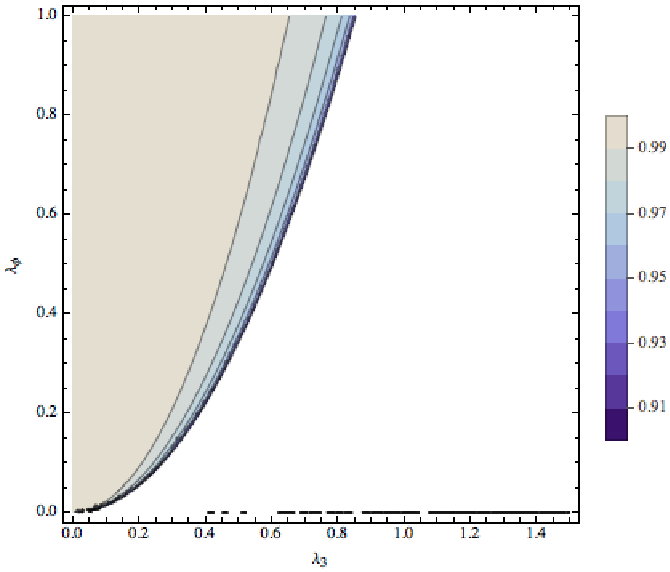

Figure 2.2: Values of $\cos\theta \geq 0.9$ as a function of λ_3 and λ_ϕ.

diagrams in Figure 2.3. The first diagram will produce a matrix element proportional to λ; the second (loop) diagram contains a logarithmic divergence in a phase space integral inside the matrix element. This can be accommodated, producing a factor of $\lambda^3/(4\pi)^2$. The ratio between successive diagrams is then $\lambda^2/(4\pi)^2$:

$$\lambda\left(1+\frac{\lambda^2}{(4\pi)^2}+...\right) \tag{2.30}$$

For the series to be perturbative then, $\lambda \ll 4\pi$.

We also might require that the branching ratio $\mathcal{B}(h' \to \phi'\phi')$ be less than or equal to the experimental limit, 0.23 (see section 1.4). This requirement generates the graph in Figure 2.4. We can see that the allowed values coincide at very low values of λ_3. We therefore choose:

$$\begin{aligned} \lambda_3 &= 0.01 \\ \lambda_\phi &= 0.5 \end{aligned} \tag{2.31}$$

which gives us a value of 0.999997 for $\cos\theta$, 0.139032 for the branching ratio, and $\Gamma(h' \to \phi'\phi') = 0.00053128$.

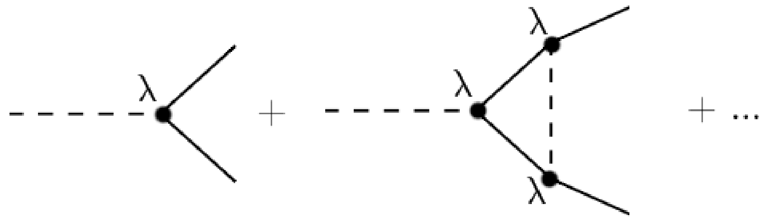

Figure 2.3: Expansion of $\Gamma(s \to \bar{f}f)$.

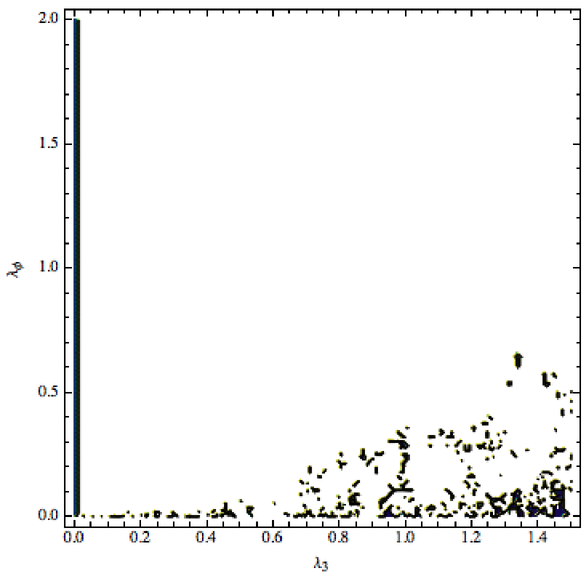

Figure 2.4: Values of λ_3 and λ_ϕ for which $\mathcal{B}(h' \to \phi'\phi') \leq 0.9$

Chapter 3

The fermion Ψ

We suppose that two non-SM fermionic fields Ψ_1 and Ψ_2 exist and are charged under $U(1)_D$. We add a Yakawa term to our Lagrangian between the two fields and our scalar field ϕ, such that the term has zero net $U(1)_D$ charge:

$$\mathcal{L}_{Yukawa} = -\lambda_\Psi \phi \overline{\Psi}_1 \Psi_2 + h.c. \tag{3.1}$$

After substituting from (2.11), we have the Lagrangian:

$$\mathcal{L}_{Yukawa} = -\frac{\lambda_\Psi}{\sqrt{2}}[\sin\theta \bar{\Psi}_1 \Psi_2 h' + \cos\theta \bar{\Psi}_1 \Psi_2 \phi' + v_\phi \bar{\Psi}_1 \Psi_2] + h.c.$$

There is coupling to both h' and ϕ' dependent on the magnitude of θ, as expected. For small θ, the fermions will interact predominantly via ϕ'.

3.1 $\Gamma(h' \to \overline{\Psi}_1 \Psi_2)$

This represents the Feynman diagram in Figure 3.1, in which the mass eigenstate h' decays into two hidden sector fermions.

Using the spinors $\bar{v}^{s_1}(p)$ and $u^{s_2}(k)$ for the outgoing $\overline{\Psi}_1$ and Ψ_2 and averaging over their initial spins, the matrix element is

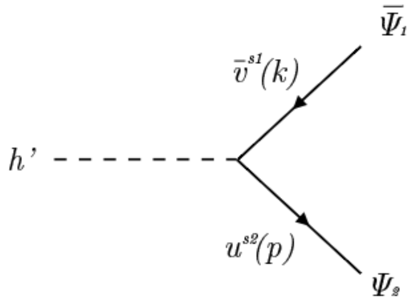

Figure 3.1: Decay of h' to $\bar{\Psi}_1$ and Ψ_2.

$$\begin{aligned}
|\mathcal{M}(h' \to \overline{\Psi}_1\Psi_2)|^2 &= \frac{\lambda_\Psi^2 \sin^2\theta}{8} \sum_{s_1,s_2} (\bar{u}^{s_2} v^{s_1})^* (\bar{u}^{s_2} v^{s_1}) \\
&= \frac{\lambda_\Psi^2 \sin^2\theta}{8} \sum_{s_1,s_2} (u_\alpha^{s_2*}\gamma^{0\alpha\beta} v_\beta^{s_1})^* (u_\mu^{s_2*}\gamma^{0\mu\nu} v_\nu^{s_1}) \\
&= \frac{\lambda_\Psi^2 \sin^2\theta}{8} \sum_{s_1,s_2} u_\alpha^{s_2}\gamma^{0\alpha\beta} v_\beta^{s_1*} u_\mu^{s_2*}\gamma^{0\mu\nu} v_\nu^{s_1}) \\
&= \frac{\lambda_\Psi^2 \sin^2\theta}{8} \left(\sum_{s_2} u_\alpha^{s_2} \bar{u}_\nu^{s_2}\right) \left(\sum_{s_1} v_\nu^{s_1} \bar{v}_\alpha^{s_1}\right) \\
&= \frac{\lambda_\Psi^2 \sin^2\theta}{8} \left(\not{p} + m_2\right)_{\alpha\nu} (\not{k} - m_1)_{\nu\alpha} \\
&= \frac{\lambda_\Psi^2 \sin^2\theta}{8} Tr\left[\left(\not{p} + m_2\right)(\not{k} - m_1)\right] \\
&= \frac{\lambda_\Psi^2 \sin^2\theta}{4} Tr\left[\not{p}\not{k} - m_1\not{p} + m_2\not{k} - m_1 m_2\right].
\end{aligned} \tag{3.3}$$

In the rest frame of the Higgs:

$$\begin{aligned}
m_h^2 &= (p+k)^2, \\
&= p^2 + k^2 + 2p.k, \\
\therefore p.k &= \frac{1}{2}(m_h^2 - m_1^2 - m_2^2).
\end{aligned} \tag{3.4}$$

Thus we have

$$
\begin{aligned}
|\mathcal{M}(h' \to \overline{\Psi}_1\Psi_2)|^2 &= \frac{\lambda_\Psi^2 \sin^2\theta}{8}(4p.k - 4m_1m_2) \\
&= \frac{\lambda_\Psi^2 \sin^2\theta}{4}(m_h^2 - m_1^2 - m_2^2 - 2m_1m_2) \\
&= \frac{\lambda_\Psi^2 \sin^2\theta}{4}(m_h^2 - (m_1+m_2)^2).
\end{aligned} \tag{3.5}
$$

Our procedure for the phase space integral is similar to that in section 2.5, except that now p^0 and k^0 are no longer identical. We again take (2.24) as a starting point.

In the Higgs' rest frame,

$$
|\mathbf{p}| = \frac{\sqrt{[m_h^2 - (m_1+m_2)^2][m_h^2 - (m_1-m_2)^2]}}{2m_h}, \tag{3.6}
$$

giving us:

$$
\begin{aligned}
\Gamma(h' \to \overline{\Psi}_1\Psi_2) &= \frac{1}{8\pi}\frac{2|\mathbf{p}|}{m_h^2}|\mathcal{M}|^2 \\
&= \frac{\lambda_\psi^2 \sin^2\theta}{32\pi m_h^3}[m_h^2 - (m_1^2 + m_2^2)]\sqrt{[m_h^2 - (m_1+m_2)^2][m_h^2 - (m_1-m_2)^2]} \\
&= \frac{\lambda_\psi^2 \sin^2\theta}{32\pi m_h^3}[m_h^2 - (m_1^2 + m_2^2)]^{\frac{3}{2}}[m_h^2 - (m_1-m_2)^2]^{\frac{1}{2}}.
\end{aligned} \tag{3.7}
$$

Note: the symmetry factor here is equal to unity since the final states are distinguishable.

This derivation would be useful when considering the case of light hidden sector fermions. For the remainder of this report, however, we will be examining the case of heavy Dark Matter, to which the Higgs does not decay.

3.2 Ψ annihilation cross sections

3.2.1 $\sigma(\bar{\Psi}_1\Psi_2 \to ss)$

We first examine the cross section of two hidden sector fermions to the scalar states ϕ' and h'.

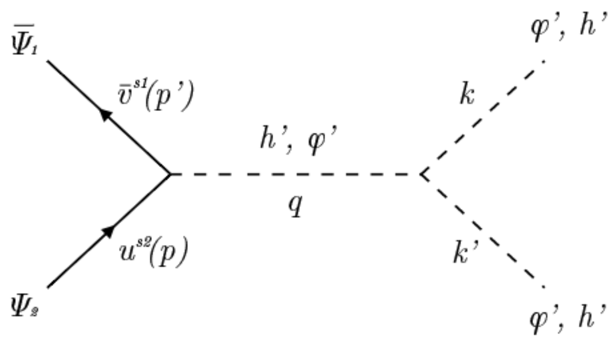

Figure 3.2: Annihilation of $\bar{\Psi}_1$ and Ψ_2 to scalar states.

Figure 3.2 represents three possible final states, each with two possible intermediate particles (i.e. six diagrams):

$$\begin{aligned}
\mathcal{M}(\bar{\Psi}_1\Psi_2 \to \phi'\phi') &= \mathcal{M}(\bar{\Psi}_1\Psi_2 \to \phi' \to \phi'\phi') + \mathcal{M}(\bar{\Psi}_1\Psi_2 \to h' \to \phi'\phi') \\
\mathcal{M}(\bar{\Psi}_1\Psi_2 \to h'h') &= \mathcal{M}(\bar{\Psi}_1\Psi_2 \to \phi' \to h'h') + \mathcal{M}(\bar{\Psi}_1\Psi_2 \to h' \to h'h') \\
\mathcal{M}(\bar{\Psi}_1\Psi_2 \to \phi'h') &= \mathcal{M}(\bar{\Psi}_1\Psi_2 \to \phi' \to \phi'h') + \mathcal{M}(\bar{\Psi}_1\Psi_2 \to h' \to \phi'h')
\end{aligned} \tag{3.8}$$

so that, for instance, contribution to the cross section for annihilation to $h'h'$ is

$$|\mathcal{M}(\bar{\Psi}_1\Psi_2 \to h'h')|^2 = |\mathcal{M}(\phi')|^2 + |\mathcal{M}(h')|^2 + \bar{\mathcal{M}}(\phi')\mathcal{M}(h') + \bar{\mathcal{M}}(h')\mathcal{M}(\phi') \tag{3.9}$$

Each diagram produces a matrix element of the general form:

$$\bar{u}^{s_1}(p')v^{s_2}(p)\frac{A_iA_j}{q^2 - m_j^2 + i\epsilon} \tag{3.10}$$

where i refers to the final states, j to the intermediate.

We can perform the same operations for the Ψ spinors as in (3.5), save that m_h is replaced with the centre-of-mass energy E_{cm} and we are now averaging over spins (i.e. we divide by 4). The propagator for the intermediate state j is also included and the vertex factors A depend on which version of diagram is under consideration. For simplicity, we assume the scattering is sufficiently off-shell to neglect the third term in the propagator.

Therefore our matrix elements (suppressing the sum and average symbols and dividing by the appropriate symmetry factors) are:

$$|\mathcal{M}(\bar{\Psi}_1\Psi_2 \to s_i s_i)|^2 = (E_{cm}^2 - (m_{\Psi_1} + m_{\Psi_2})^2)$$
$$\left[\frac{A_{\bar{\Psi}\Psi h}^2 A_{hii}^2}{2(E_{cm}^2 - m_h^2)^2} + \frac{A_{\bar{\Psi}\Psi\phi}^2 A_{\phi ii}^2}{2(E_{cm}^2 - m_\phi^2)^2} + \frac{A_{\bar{\Psi}\Psi h} A_{hii} A_{\bar{\Psi}\Psi\phi} A_{\phi ii}}{(E_{cm}^2 - m_h^2)(E_{cm}^2 - m_\phi^2)}\right] \tag{3.11}$$

and

$$|\mathcal{M}(\bar{\Psi}_1\Psi_2 \to h'\phi')|^2 = (E_{cm}^2 - (m_{\Psi_1} + m_{\Psi_2})^2)$$
$$\left[\frac{A_{\bar{\Psi}\Psi h}^2 A_{hh\phi}^2}{2(E_{cm}^2 - m_h^2)^2} + \frac{A_{\bar{\Psi}\Psi\phi}^2 A_{h\phi\phi}^2}{2(E_{cm}^2 - m_\phi^2)^2} + \frac{A_{\bar{\Psi}\Psi h} A_{hh\phi} A_{\bar{\Psi}\Psi\phi} A_{h\phi\phi}}{(E_{cm}^2 - m_h^2)(E_{cm}^2 - m_\phi^2)}\right] \tag{3.12}$$

where the vertex factors A are given in Figures 9 and 8.

The cross section 1.27 is:

$$\begin{aligned}
d\sigma &= \frac{|\mathcal{M}|^2}{4v_{rel}E_1E_2}\frac{1}{(2\pi)^2}\delta^{(4)}((p+p') - (k+k'))\frac{d^3k}{2E_3}\frac{d^3k'}{2E_4} \\
&= \frac{|\mathcal{M}|^2}{4v_{rel}E_1E_2}\frac{1}{(2\pi)^2}\delta((E_1+E_2) - (E_3+E_4))\frac{d^3k}{4E_3E_4} \\
&= \frac{|\mathcal{M}|^2}{4v_{rel}E_1E_2}\frac{|\mathbf{k}|}{(2\pi)^2}\delta\left(|\mathbf{k}| - \frac{\sqrt{(E_{cm}^2 - (m_3+m_4)^2)(E_{cm}^2 - (m_3-m_4)^2)}}{2E_{cm}}\right)\frac{d|\mathbf{k}|d\Omega}{4(E_3+E_4)}
\end{aligned} \tag{3.13}$$

We can use:

$$4v_{rel}E_1E_2 = 2\sqrt{(E_{cm}^2 - (m_1+m_2)^2)(E_{cm}^2 - (m_1-m_2)^2)} \tag{3.14}$$

giving us:

$$\sigma(\bar{\Psi}_1\Psi_2 \to h'h') = \frac{\sqrt{E_{cm}^2 - 4m_h^2}}{32\pi E_{cm}} \sqrt{\frac{E_{cm}^2 - (m_{\Psi_1} + m_{\Psi_2})^2}{E_{cm}^2 - (m_{\Psi_1} - m_{\Psi_2})^2}} \left[\frac{A_{\bar{\Psi}\Psi h}^2 A_{hhh}^2}{2(E_{cm}^2 - m_h^2)^2} + \frac{A_{\bar{\Psi}\Psi\phi}^2 A_{\phi hh}^2}{2(E_{cm}^2 - m_\phi^2)^2} + \frac{A_{\bar{\Psi}\Psi h} A_{hhh} A_{\bar{\Psi}\Psi\phi} A_{\phi hh}}{(E_{cm}^2 - m_h^2)(E_{cm}^2 - m_\phi^2)} \right] \tag{3.15}$$

$$\sigma(\bar{\Psi}_1\Psi_2 \to \phi'\phi') = \frac{\sqrt{E_{cm}^2 - 4m_\phi^2}}{32\pi E_{cm}} \sqrt{\frac{E_{cm}^2 - (m_{\Psi_1} + m_{\Psi_2})^2}{E_{cm}^2 - (m_{\Psi_1} - m_{\Psi_2})^2}} \left[\frac{A_{\bar{\Psi}\Psi h}^2 A_{h\phi\phi}^2}{2(E_{cm}^2 - m_\phi^2)^2} + \frac{A_{\bar{\Psi}\Psi\phi}^2 A_{\phi hh}^2}{2(E_{cm}^2 - m_\phi^2)^2} + \frac{A_{\bar{\Psi}\Psi h} A_{h\phi\phi} A_{\bar{\Psi}\Psi\phi} A_{\phi hh}}{(E_{cm}^2 - m_h^2)(E_{cm}^2 - m_\phi^2)} \right] \tag{3.16}$$

$$\sigma(\bar{\Psi}_1\Psi_2 \to h'\phi') = \frac{\sqrt{(E_{cm}^2 - (m_\phi + m_h)^2)(E_{cm}^2 - (m_\phi - m_h)^2)}}{16\pi E_{cm}^2} \sqrt{\frac{E_{cm}^2 - (m_{\Psi_1} + m_{\Psi_2})^2}{E_{cm}^2 - (m_{\Psi_1} - m_{\Psi_2})^2}} \left[\frac{A_{\bar{\Psi}\Psi h}^2 A_{hh\phi}^2}{2(E_{cm}^2 - m_h^2)^2} + \frac{A_{\bar{\Psi}\Psi\phi}^2 A_{h\phi\phi}^2}{2(E_{cm}^2 - m_\phi^2)^2} + \frac{A_{\bar{\Psi}\Psi h} A_{h\phi\phi} A_{\bar{\Psi}\Psi\phi} A_{h\phi\phi}}{(E_{cm}^2 - m_h^2)(E_{cm}^2 - m_\phi^2)} \right] \tag{3.17}$$

where we have divided by the appropriate symmetry factor depending on whether the final states are identical.

3.2.2 $\sigma(\bar{\Psi}_1\Psi_2 \to f\bar{f})$

Figure 3.3 represents two diagrams, one for each intermediate state, so that

$$|\mathcal{M}(\bar{\Psi}_1\Psi_2 \to f\bar{f})|^2 = |\mathcal{M}(h')|^2 + |\mathcal{M}(\phi')|^2 + \bar{\mathcal{M}}(h')\mathcal{M}(\phi') + \bar{\mathcal{M}}(\phi')\mathcal{M}(h') \tag{3.18}$$

Summing over the spins of the final states and averaging over the initial (with q^2 set to E_{cm}^2):

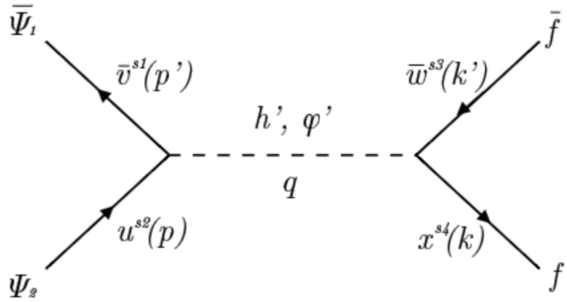

Figure 3.3: Annihilation of $\bar{\Psi}_1$ and Ψ_2 to fermion states.

$$
\begin{aligned}
|\mathcal{M}(s_i)|^2 &= \frac{A^2_{\bar{\Psi}\Psi i}A^2_{i\bar{f}f}}{4(E^2_{cm}-m_i^2)^2}\sum_{s_1,s_2,s_3,s_4}(\bar{v}^{s_1}u^{s_2})(\bar{w}^{s_3}x^{s_4})^*(\bar{v}^{s_1}u^{s_2})^*(\bar{w}^{s_3}x^{s_4}) \\
&= \frac{A^2_{\bar{\Psi}\Psi i}A^2_{i\bar{f}f}}{4(E^2_{cm}-m_i^2)^2}\sum_{s_1,s_2,s_3,s_4}(v^{s_1*}_\alpha\gamma^{0\alpha\beta}u^{s_2}_\beta)(w^{s_3}_\mu\gamma^{0\mu\nu}x^{s_4*}_\nu)(v^{s_1}_\delta\gamma^{0\delta\epsilon}u^{s_2*}_\epsilon)(w^{s_3*}_\eta\gamma^{0\eta\iota}x^{s_4}_\iota) \\
&= \frac{A^2_{\bar{\Psi}\Psi i}A^2_{i\bar{f}f}}{4(E^2_{cm}-m_i^2)^2}\sum_{s_1,s_2,s_3,s_4}(v^{s_1}_\delta v^{s_1*}_\alpha\gamma^{0\alpha\beta})(u^{s_2}_\beta\gamma^{0\delta\epsilon}u^{s_2*}_\epsilon)(w^{s_3}_\mu w^{s_3*}_\eta\gamma^{0\eta\iota})(x^{s_4}_\iota\gamma^{0\mu\nu}x^{s_4*}_\nu) \\
&= \frac{A^2_{\bar{\Psi}\Psi i}A^2_{i\bar{f}f}}{4(E^2_{cm}-m_i^2)^2}\left(\sum_{s_1}v^{s_1}_\delta\bar{v}^{s_1}_\beta\right)\left(\sum_{s_2}u^{s_2}_\beta\bar{u}^{s_2}_\delta\right)\left(\sum_{s_3}w^{s_3}_\mu\bar{w}^{s_3}_\iota\right)\left(\sum_{s_4}x^{s_4}_\iota\bar{x}^{s_4}_\mu\right) \\
&= \frac{A^2_{\bar{\Psi}\Psi i}A^2_{i\bar{f}f}}{4(E^2_{cm}-m_i^2)^2}(\not{p}'-m_1)_{\delta\beta}\left(\not{p}+m_2\right)_{\beta\delta}\left(\not{k}'-m_3\right)_{\mu\iota}(\not{k}+m_4)_{\iota\mu} \\
&= \frac{A^2_{\bar{\Psi}\Psi i}A^2_{i\bar{f}f}}{4(E^2_{cm}-m_i^2)^2}Tr\left[(\not{p}'-m_1)\left(\not{p}+m_2\right)\right]Tr\left[\left(\not{k}'-m_3\right)(\not{k}+m_4)\right] \\
&= \frac{A^2_{\bar{\Psi}\Psi i}A^2_{i\bar{f}f}}{4(E^2_{cm}-m_i^2)^2}Tr\left[\not{p}'\not{p}-m_1\not{p}+m_2\not{p}'-m_1m_2\right]Tr\left[\not{k}'\not{k}-m_3\not{k}+m_4\not{k}'-m_3m_4\right] \\
&= \frac{A^2_{\bar{\Psi}\Psi i}A^2_{i\bar{f}f}}{4(E^2_{cm}-m_i^2)^2}(4p.p'-4m_1m_2)(4k.k'-4m_3m_4) \\
&= \frac{A^2_{\bar{\Psi}\Psi i}A^2_{i\bar{f}f}}{(E^2_{cm}-m_i^2)^2}(E^2_{cm}-m_1^2-m_2^2-2m_1m_2)(E^2_{cm}-m_3^2-m_4^2-2m_3m_4) \\
&= \frac{A^2_{\bar{\Psi}\Psi i}A^2_{i\bar{f}f}}{(E^2_{cm}-m_i^2)^2}(E^2_{cm}-(m_1+m_2)^2)(E^2_{cm}-(m_3+m_4)^2)
\end{aligned}
\tag{3.19}
$$

where $A_{\bar{\Psi}\Psi i}$ is given in Figure 8, $m_3 = m_4 = m_f$ and $A_{i\bar{f}f}$ is the usual SM coupling of the Higgs to the fermions (m_f/v_h), multiplied by $\cos\theta$ if the $i = h'$ and $\sin\theta$ if $i = \phi'$, so that

$$A_{\bar{\Psi}\Psi\phi}A_{\phi\bar{f}f} = A_{\bar{\Psi}\Psi h}A_{h\bar{f}f} = \frac{\lambda_\Psi m_f}{2\sqrt{2}v_h}\sin 2\theta \tag{3.20}$$

As $m_3 = m_4 = m_f$, the entire matrix element simplifies slightly to:

$$|\mathcal{M}(\bar{\Psi}_1\Psi_2 \to f\bar{f})|^2 = \frac{\lambda_\Psi^2 m_f^2 \sin^2 2\theta}{8v_h^2}(E_{cm}^2 - (m_{\Psi_1} + m_{\Psi_2})^2)(E_{cm}^2 - 4m_f^2) \left[\frac{1}{(E_{cm}^2 - m_h^2)^2} + \frac{1}{(E_{cm}^2 - m_\phi^2)^2} + \frac{2}{(E_{cm}^2 - m_h^2)(E_{cm}^2 - m_\phi^2)}\right] \tag{3.21}$$

The integral over phase space proceeds as before, giving us the decay cross section:

$$\sigma(\bar{\Psi}_1\Psi_2 \to f\bar{f}) = \frac{\lambda_\Psi^2 m_f^2 \sin^2 2\theta}{128\pi v_h^2 E_{cm}}\sqrt{\frac{E_{cm}^2 - (m_{\Psi_1} + m_{\Psi_2})^2}{E_{cm}^2 - (m_{\Psi_1} - m_{\Psi 2})^2}}(E_{cm}^2 - 4m_f^2)^{3/2} \left[\frac{1}{(E_{cm}^2 - m_h^2)^2} + \frac{1}{(E_{cm}^2 - m_\phi^2)^2} + \frac{2}{(E_{cm}^2 - m_h^2)(E_{cm}^2 - m_\phi^2)}\right] \tag{3.22}$$

3.2.3 $\sigma(\bar{\Psi}_1\Psi_2 \to V\bar{V})$

Again, Figure 3.4 represents two sets of two diagrams:

$$|\mathcal{M}(\bar{\Psi}_1\Psi_2 \to V\bar{V})|^2 = |\mathcal{M}(h')|^2 + |\mathcal{M}(\phi')|^2 + \bar{\mathcal{M}}(h')\mathcal{M}(\phi') + \bar{\mathcal{M}}(\phi')\mathcal{M}(h') \tag{3.23}$$

where $V = W, Z$.

Summing over boson polarisation states ϵ, averaging over fermion spins and using the identity

$$\sum_{\lambda=0,\pm}(\epsilon_\mu^\lambda(p))^*\epsilon_\nu^\lambda(p) = -g_{\mu\nu} + \frac{p_\mu p_\nu}{M^2}, \tag{3.24}$$

we have the general expression

$$\begin{aligned}
|\mathcal{M}(s_i)|^2 &= \frac{A^2_{\bar\Psi\Psi i}A^2_{\bar V V i}}{4(E^3_{cm}-m_i^2)^2}\sum_{s_1,s_2}\sum_{\substack{\lambda_1=0,\pm\\ \lambda_2=0,\pm}}\bar v^{s_1}u^{s_2}\epsilon_\mu^{\lambda_1 *}(k)\epsilon_\nu^{\lambda_2}(k')g_{\mu\nu}g^{\alpha\beta}\epsilon_\alpha^{\lambda_1}(k)\epsilon_\beta^{\lambda_2 *}(k')(\bar v^{s_1}u^{s_2})^* \\
&= \frac{A^2_{\bar\Psi\Psi i}A^2_{\bar V V i}(E^2_{cm}-(m_1+m_2)^2)}{2(E^3_{cm}-m_i^2)^2} \\
&\qquad g_{\mu\nu}g^{\alpha\beta}\left(\sum_{\lambda_1=0,\pm}(\epsilon_\mu^{\lambda_1}(k))^*\epsilon_\alpha^{\lambda_1}(k)\right)\left(\sum_{\lambda_2=0,\pm}(\epsilon_\nu^{\lambda_2}(k'))^*\epsilon_\beta^{\lambda_2}(k')\right) \\
&= \frac{A^2_{\bar\Psi\Psi i}A^2_{\bar V V i}(E^2_{cm}-(m_1+m_2)^2)}{2(E^3_{cm}-m_i^2)^2} \\
&\qquad g_{\mu\nu}g^{\alpha\beta}\left(-g_{\mu\alpha}+\frac{k_\mu k_\alpha}{m_V^2}\right)\left(-g_{\nu\beta}+\frac{k'_\nu k'_\beta}{m_V^2}\right) \\
&= \frac{A^2_{\bar\Psi\Psi i}A^2_{\bar V V i}(E^2_{cm}-(m_1+m_2)^2)}{2(E^3_{cm}-m_i^2)^2} \\
&\qquad g_{\mu\nu}g^{\alpha\beta}\left(g_{\mu\alpha}g_{\nu\beta}-g_{\mu\alpha}\frac{k'_\nu k'_\beta}{m_V^2}-g_{\nu\beta}\frac{k_\mu k_\alpha}{m_V^2}+\frac{k_\mu k_\alpha k'_\nu k'_\beta}{m_V^4}\right) \\
&= \frac{A^2_{\bar\Psi\Psi i}A^2_{\bar V V i}(E^2_{cm}-(m_1+m_2)^2)}{2(E^3_{cm}-m_i^2)^2}\left[4-\frac{k'^2}{m_V^2}-\frac{k^2}{m_V^2}+\frac{k.k'}{m_V^4}\right] \\
&= \frac{A^2_{\bar\Psi\Psi i}A^2_{\bar V V i}(E^2_{cm}-(m_1+m_2)^2)}{2(E^3_{cm}-m_i^2)^2}\left[2-\frac{E^4_{cm}+4m_V^4-4E^2_{cm}m_V^2}{4m_V^4}\right] \\
&= \frac{A^2_{\bar\Psi\Psi i}A^2_{\bar V V i}(E^2_{cm}-(m_1+m_2)^2)}{2(E^3_{cm}-m_i^2)^2}\left[3+\frac{E^4_{cm}}{4m_V^4}-\frac{E^2_{cm}}{m_V^2}\right]
\end{aligned} \tag{3.25}$$

where the vertex factor $A_{\bar V V i}$ is the usual SM $2m_V^2/v_h$ multiplied by a trig function, and in analogy to (3.20), the product of vertex factors is given by

$$A_{\bar\Psi\Psi\phi}A_{\bar V V\phi} = A_{\bar\Psi\Psi h}A_{\bar V V h} = \frac{\lambda_\Psi m_V^2}{\sqrt{2}v_h}\sin 2\theta \tag{3.26}$$

so that our final matrix element contribution is

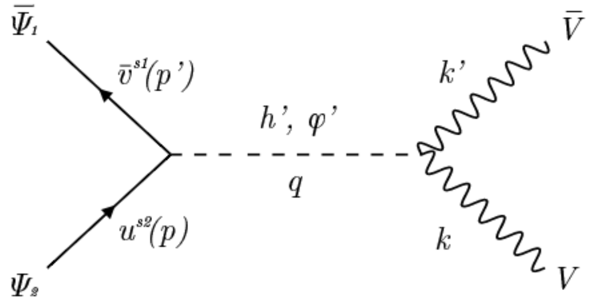

Figure 3.4: Annihilation of $\bar{\Psi}_1$ and Ψ_2 to weak bosons.

$$|\mathcal{M}(\bar{\Psi}_1\Psi_2 \to V\bar{V})|^2 = \frac{\lambda_\Psi^2 m_V^4 \sin^2 2\theta (E_{cm}^2 - (m_1+m_2)^2)}{4v_h^2}\left[3 + \frac{E_{cm}^4}{4m_V^4} - \frac{E_{cm}^2}{m_V^2}\right] \left[\frac{1}{(E_{cm}^2 - m_h^2)^2} + \frac{1}{(E_{cm}^2 - m_\phi^2)^2} + \frac{2}{(E_{cm}^2 - m_h^2)(E_{cm}^2 - m_\phi^2)}\right] \tag{3.27}$$

Finally, we have as before

$$\sigma(\bar{\Psi}_1\Psi_2 \to V\bar{V}) = \frac{\lambda_\Psi^2 m_V^4 \sin^2 2\theta}{64\pi v_h^2 E_{cm}}\sqrt{E_{cm}^2 - 4m_V^2}\sqrt{\frac{E_{cm}^2 - (m_{\Psi_1}+m_{\Psi_2})^2}{E_{cm}^2 - (m_{\Psi_1}-m_{\Psi_2})^2}} \left[3 + \frac{E_{cm}^4}{4m_V^4} - \frac{E_{cm}^2}{m_V^2}\right]\left[\frac{1}{(E_{cm}^2 - m_h^2)^2} + \frac{1}{(E_{cm}^2 - m_\phi^2)^2} + \frac{2}{(E_{cm}^2 - m_h^2)(E_{cm}^2 - m_\phi^2)}\right], \tag{3.28}$$

divided by a symmetry factor $S = 2$ for the annihilation to ZZ.

3.3 Cross section ratios

For the sake of convenience, we approximate $m_1 = m_2 = m_\Psi$, so that our cross sections are given by:

$$\sigma(\bar{\Psi}_1\Psi_2 \to h'h') = \frac{\sqrt{E_{cm}^2 - 4m_h^2}}{32\pi E_{cm}^2}\sqrt{E_{cm}^2 - 4m_\Psi^2}\left[\frac{A_{\bar{\Psi}\Psi h}^2 A_{hhh}^2}{2(E_{cm}^2 - m_h^2)^2} + \frac{A_{\bar{\Psi}\Psi\phi}^2 A_{\phi hh}^2}{2(E_{cm}^2 - m_\phi^2)^2} + \frac{A_{\bar{\Psi}\Psi h}A_{hhh}A_{\bar{\Psi}\Psi\phi}A_{\phi hh}}{(E_{cm}^2 - m_h^2)(E_{cm}^2 - m_\phi^2)}\right] \tag{3.29}$$

$$\sigma(\bar{\Psi}_1\Psi_2 \to \phi'\phi') = \frac{\sqrt{E_{cm}^2 - 4m_\phi^2}}{32\pi E_{cm}^2}\sqrt{E_{cm}^2 - 4m_\Psi^2}\left[\frac{A_{\bar{\Psi}\Psi h}^2 A_{h\phi\phi}^2}{2(E_{cm}^2 - m_\phi^2)^2} + \frac{A_{\bar{\Psi}\Psi\phi}^2 A_{\phi hh}^2}{2(E_{cm}^2 - m_\phi^2)^2} + \frac{A_{\bar{\Psi}\Psi h}A_{h\phi\phi}A_{\bar{\Psi}\Psi\phi}A_{\phi hh}}{(E_{cm}^2 - m_h^2)(E_{cm}^2 - m_\phi^2)}\right] \tag{3.30}$$

$$\sigma(\bar{\Psi}_1\Psi_2 \to h'\phi') = \frac{\sqrt{(E_{cm}^2 - (m_\phi + m_h)^2)(E_{cm}^2 - (m_\phi - m_h)^2)}}{16\pi E_{cm}^3}\sqrt{E_{cm}^2 - 4m_\Psi^2}\left[\frac{A_{\bar{\Psi}\Psi h}^2 A_{hh\phi}^2}{2(E_{cm}^2 - m_h^2)^2} + \frac{A_{\bar{\Psi}\Psi\phi}^2 A_{h\phi\phi}^2}{2(E_{cm}^2 - m_\phi^2)^2} + \frac{A_{\bar{\Psi}\Psi h}A_{h\phi\phi}A_{\bar{\Psi}\Psi\phi}A_{h\phi\phi}}{(E_{cm}^2 - m_h^2)(E_{cm}^2 - m_\phi^2)}\right] \tag{3.31}$$

$$\sigma(\bar{\Psi}_1\Psi_2 \to \bar{f}f) = \frac{\lambda_\Psi^2 m_f^2 \sin^2 2\theta}{128\pi v_h^2 E_{cm}^2}\sqrt{\frac{E_{cm}^2 - 4m_f^2}{E_{cm}^2 - 4m_\Psi^2}} \tag{3.32}$$

$$\sigma(\bar{\Psi}_1\Psi_2 \to WW*) = \frac{\lambda_\Psi^2 m_V^4 \sin^2 2\theta}{64\pi v_h^2 E_{cm}^2}\sqrt{\frac{E_{cm}^2 - 4m_W^2}{E_{cm}^2 - 4m_\Psi^2}} \tag{3.33}$$

$$\sigma(\bar{\Psi}_1\Psi_2 \to ZZ) = \frac{\lambda_\Psi^2 m_V^4 \sin^2 2\theta}{128\pi v_h^2 E_{cm}^2}\sqrt{\frac{E_{cm}^2 - 4m_Z^2}{E_{cm}^2 - 4m_\Psi^2}} \tag{3.34}$$

We then have two free parameters - λ_Ψ and the mass of Ψ, which however do not affect the cross section ratios, which are plotted in Figure 3.5.

As can be easily seen from Figure 3.5, the dominant annihilation channel of the $\bar{\Psi}\Psi$ interaction is that to $h'\phi'$, followed closely by $\phi'\phi'$ (seen more closely in Figure 3.6) and lagged by a long way by $h'h'$. We notice that in limits of small θ:

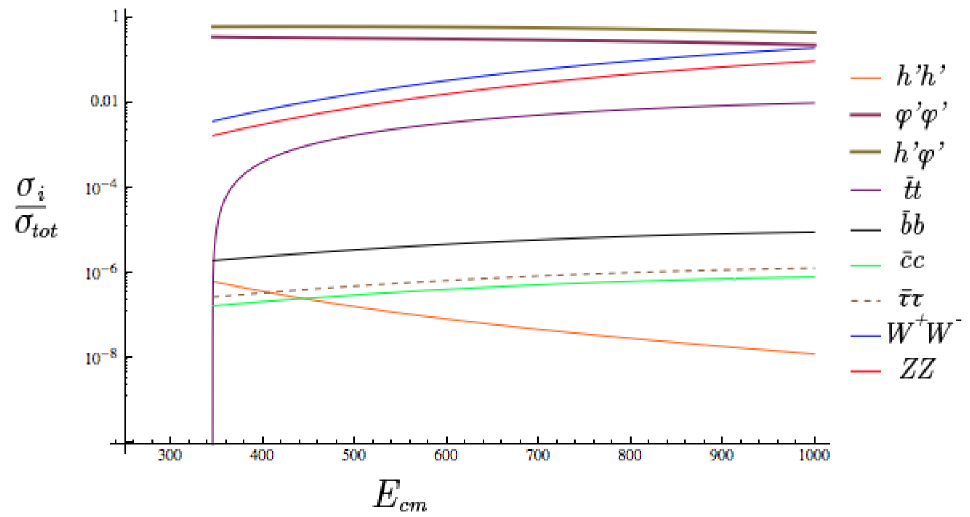

Figure 3.5: Cross section ratios of the annihilation of two Ψs to SM particles and scalars as a function of centre-of-mass energy ($m_\Psi = 100$ GeV).

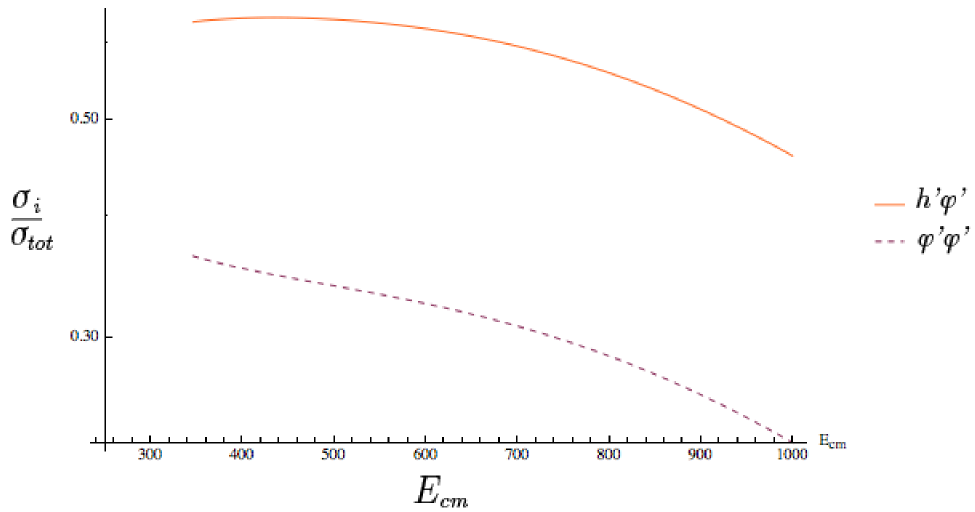

Figure 3.6: Cross section ratios of the annihilation of two Ψs to scalars $\phi'\phi'$ and $h'\phi'$ ($m_\Psi = 100$ GeV).

$$
\begin{aligned}
A_{hhh} &\approx 2v_h\lambda_h \\
A_{\phi\phi\phi} &\approx 2v_\phi\lambda_\phi \\
A_{hh\phi} &\approx (v_\phi\lambda_3)/2 \\
A_{h\phi\phi} &\approx (v_h\lambda_3)/2
\end{aligned}
\tag{3.35}
$$

Due to the negligible coupling of Ψ to h' in this limit, one can approximate the cross sections to include only those due to an intermediate ϕ. In this case:

$$
\begin{aligned}
\sigma(\rightarrow h'h') &\propto \lambda_\Psi^2 v_\phi^2 \lambda_3^2 \\
\sigma(\rightarrow \phi'\phi') &\propto \lambda_\Psi^2 v_\phi^2 \lambda_\phi^2 \\
\sigma(\rightarrow h'\phi') &\propto \lambda_\Psi^2 v_h^2 \lambda_3^2
\end{aligned}
\tag{3.36}
$$

It can be seen that while decays to both $h'h'$ and $h'\phi'$ are suppressed by our choice of a small λ_3, the decay to $h'\phi'$ is promoted by its dependence on the large Higgs vev.

3.4 The relic abundance of Ψ

3.4.1 Expanding $\langle\sigma v_{rel}\rangle$

Assuming that freeze-out occurs after Ψ has become non-relativistic (see section 1.5.1), we can expand the $\langle\sigma v_{rel}\rangle$ by substituting E_{cm} with an expression in terms of v_{rel}:

$$
\begin{aligned}
E_{cm} &= 2E_\Psi = 2\gamma_\Psi m_\Psi \\
&= \frac{2m_\Psi}{\sqrt{1-v_\Psi^2}} \\
&= \frac{2m_\Psi}{\sqrt{1-\frac{v_{rel}^2}{4}}}
\end{aligned}
\tag{3.37}
$$

where we have made the non-relativistic substitution $v_{rel} = 2v_\Psi$.

3.4.2 Choosing parameters

In order to calculate the current DM mass density, we choose the mass of our fermion such that

$$\begin{aligned} m_\Psi &= 100 \text{ GeV}, \\ T_f &= \frac{m_\Psi}{25} = 4 \text{ GeV}, \\ \text{and} \\ x_f &= 25. \end{aligned} \tag{3.38}$$

With these values, the DM would have been frozen out long before any other particle species. Therefore,

$$g_* = g_{*S} = 75.75. \tag{3.39}$$

Where we have included the degrees of freedom listed in table 3.1 - omitting ϕ', t and h', which would not be relativistic at this temperature.

Particle	*Mass*	g_i
photon	0	2
gluon	0	16
$u, \bar{u}$	3 MeV	12
$d, \bar{d}$	6 MeV	12
$s, \bar{s}$	100 MeV	12
$c, \bar{c}$	1.2 GeV	12
e^+, e^-	0.511 MeV	4
μ^+, μ^-	105.7 MeV	4
τ^+, τ^-	1.777 GeV	4
$\nu_e, \bar{\nu_e}$	3 eV	2
$\nu_\mu, \bar{\nu_\mu}$	0.19 MeV	2
$\nu_\tau, \bar{\nu_\tau}$	18.2 MeV	2
	TOTAL	**75.75**

Table 3.1: Relativistic degrees of freedom in the early universe at $T \approx 4$ GeV.

Expanding each cross section in turn, we find that all of the annihilations take place via p-wave interactions. Therefore we have no hesitation in adding together all the kinematically-allowed cross sections (i.e. excluding those to $h'h'$ and $\bar{t}t$),

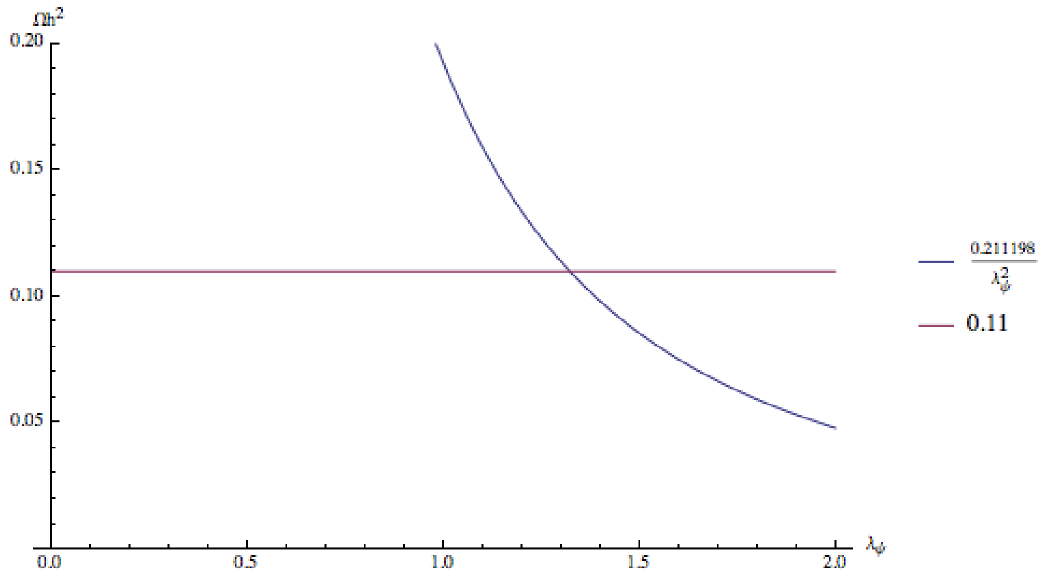

Figure 3.7: Comparison between calculated Ωh^2 and the observed value.

and expanding similarly. Substituting our fixed parameters, we obtain

$$\langle \sigma v \rangle = 1.37026 \times 10^{-9} \lambda_\Psi^2 v_{rel}^2 + \mathcal{O}(v_{rel}^4). \tag{3.40}$$

Substituting all these values into equations 1.32 and 1.33, we obtain:

$$\begin{aligned} Y_\infty &= \frac{6.81642 \times 10^{-12}}{\lambda_\Psi^2} \\ \Omega h^2 &= \frac{0.192223}{\lambda_\Psi^2} \end{aligned} \tag{3.41}$$

We find (see Figure 3.7) that $\Omega h^2 = 0.11$ when $\lambda_\Psi = 1.32192$. This latter value satisfies the condition of being small enough in comparison to 4π to suppress loop diagrams and allow for perturbative expansions of the interactions.

Conclusion

The aim of this project was to gain familiarity with a few of the basic techniques and concepts of theoretical particle physics, and then to apply them to a toy model and see them in practice. While reading of the standard texts and recent papers was helpful in outlining the theory, the best demonstration of the physics involved was the working out, by hand and on computer, the effects of introducing vacuum expectation values and extra fields and couplings. In addition, the investigation was driven forward by the existence of a definite goal - that of proposing a new Dark Matter candidate.

We supposed a non-SM symmetry $U(1)_D$ under which a complex scalar field ϕ transformed, and gauging it with coupling constant g_D. The first task was to introduce a potential dependent on the Higgs field H and ϕ, with a term mixing the two. This potential contained 5 free parameters (to add to the parameter g_D), two of mass dimension and three dimensionless. Both fields developed vacuum expectation values which produced mass terms for the electroweak bosons and the boson of $U(1)_D$, Z'. For the sake of argument, we dismissed g_D as extremely small (see discussion below). After choosing the unitary gauge, we diagonalised the $h - \phi_r$ system and observed coupling between the mass eigenstate ϕ' and the particles of the SM.

We identified h' with the SM Higgs (giving us the SM values for v_h and m_h), and chose a value for ϕ' of 20 GeV, allowing us to solve for three parameters. We then calculated the decay rate of $h' \to \phi'\phi'$ in terms of the remaining two, and imposed two further conditions: that the branching ratio not exceed that calculated by others for Higgs decays to invisible states, and that the mixing angle between h and ϕ_r be extremely small, to be in accord with measurements. By taking into account the requirement of perturbativity, we were able to make a reasonable choice for the last two parameters.

We proposed further fermionic fields Ψ_1 and Ψ_2, also charged under $U(1)_D$, which coupled to ϕ in a Yakawa interaction, and thus to ϕ' and h'. The Ψ fermions could therefore interact with the particles of the SM in decay and annihilation processes through the scalar states - the 'Higgs portal' approach. After calculating the decay width of $h' \to \bar{\Psi}_1\Psi_2$ as a function of the Ψ fermion masses, we selected a mass of 100 GeV (forbidding the aforementioned decay) and calculated the annihilation cross sections to h', ϕ', fermions and electroweak bosons, as a function of the Yakawa coupling parameter λ_Ψ.

We used these values to show that all the annihilations were p-wave interactions, and calculated the relic abundance of the Ψ fermions, with a freeze-out temperature of 4 GeV. Using this result, we calculated the mass density as a function of λ_Ψ and compared it with the observed value for Dark Matter. We found that we could fit our model to observations with a reasonable value of λ_Ψ.

Any student, when learning of the Standard Model and its symmetry groups, must wonder if there are any further symmetries and fields out there, and what effect the existence of such would have on the universe. We have shown here that it is extremely fruitful to model these effects, constraining the parameters of our model by reference to observations, as a method of approach to explore one of the biggest areas of modern research - the search for Dark Matter.

Avenues of further investigation

It would be interesting to experiment with differing the masses of ϕ' and Ψ to look at more extreme cases for the parameters. If we made $m_\phi > 2m_h$, however, we would lose the constraint provided by requiring the $\mathcal{B}(h' \to \phi'\phi') < 0.23$ (see section 2.5.1).

One of the grander assumptions we made was that the charge g_D of ϕ under $U(1)_D$ was very small. This allowed us to neglect all discussion of the $U(1)_D$ gauge boson, Z'_μ. Indeed, g_D would need to be extremely small to make this approximation, as the mass of Z'_μ is equal to $g_D v_\phi$, where $v_\phi = 28$ GeV in this parameterisation. Raising the value of g_D would enable access to a new range of interactions via a coupling of Ψ to Z'_μ, including direct production of Z'_μ at the LHC, providing very strict further constraints on our parameters. The dynamics of DM freeze-out would also be affected.

Another phenomenon worthy of investigation is that of kinematic mixing. As described in section 1.1, gauge bosons have a kinetic term of the form $F_{\mu\nu}$, which is gauge invariant in itself, but that the Lagrangian must have terms of the form $F_{\mu\nu}F^{\mu\nu}$ in order to be Lorentz invariant. Thus a term mixing the kinetic terms of two different gauge bosons would be both gauge and Lorentz invariant. For example we could introduce a term between an electroweak $F_{\mu\nu}$ term and that of our hidden gauge boson $K_{\mu\nu}$:

$$\mathcal{L}_{KM} = -\frac{1}{4}F_{\mu\nu}K^{\mu\nu} \tag{3.42}$$

When expanded (see equation 1.9), this would give mixing between the two bosons. After diagonalising this system, we could make corrections to the mass of the SM boson. By requiring that the mass remain within current precision of the measured value, we can place a further restriction on the parameters.

It may also be fruitful to propose additional hidden symmetries of $SU(2)$ and $SU(3)$ under which more interesting forms of hidden fields might transform.

References

[1] G Belanger, B Dumont, U Ellwanger, JF Gunion, and S Kraml. Status of invisible Higgs decays. *arXiv:1302.5694v3*, 2013.

[2] G. Bertone, D. Hooper, and J. Silk. Particle Dark Matter: Evidence, candidates and constraints. *arXiv:hep-ph/0404175v2*, 2008.

[3] G Bhattacharyya, D Das, PB Pal, and MN Rebelo. Scalar sector properties of two-Higgs-doublet models with a global U(1) symmetry. *arXiv:1308.4297*, 2013.

[4] The ATLAS Collaboration. Measurements of the Higgs boson production and decay rates and coupling strengths using pp collision data at $\sqrt{s} = 7$ and 8 TeV in the ATLAS experiment. *arXiv:1507.04548v1*, 2015.

[5] The CMS Collaboration. Evidence for the direct decay of the 125 GeV Higgs boson to fermions. *Nature Physics: Letters*, 10, 2014.

[6] Wan-Lei Guo and Yue-Liang Wu. The real singlet scalar dark matter model. *arXiv:1006.2518*, 2010.

[7] R Kappl, M Ratz, and MW Winkler. Light dark matter in the singlet-extended MSSM. *arXiv:1010.0553*, 2010.

[8] EW Kolb and MS Turner. *The Early Universe*. Addison-Wesley, 1990.

[9] D Majumdar. *Dark Matter: An Introduction*. Taylor & Francis, 2015.

[10] B Patt and F Wilczek. Higgs-field portal into hidden sectors. *arXiv:hep-ph/0605188*, 2006.

[11] ME Peskin and DV Shroeder. *An Introduction to Quantum Field Theory*. Westview Press, 1995.

[12] L Reina. TASI 2011: Lectures on Higgs-Boson Physics. *arXiv:1208.5504*, 2011.

[13] R Schabinger and JD Wells. A minimal spontaneously broken hidden sector and its impact on Higgs boson physics at the Large Hadron Collider. *arXiv:hep-ph/0509209*, 2005.

Appendix A: θ

$$
\begin{aligned}
\theta = \tan^{-1}\Bigg[\frac{1}{\lambda_3 v_h v_\phi}\Bigg(&\frac{1}{4}\left(-2\mu_h^2 + 6\lambda_h v_h^2 + \lambda_3 v_\phi^2\right) + \frac{1}{4}\left(-\lambda_3 v_h^2 + 2\mu_\phi^2 - 6\lambda_\phi v_\phi^2\right) \\
&+ \sqrt{\frac{1}{4}\left(-2\mu_h^2 + 6\lambda_h v_h^2 + \lambda_3 v_\phi^2\right) + \frac{1}{4}\left(-\lambda_3 v_h^2 + 2\mu_\phi^2 - 6\lambda_\phi v_\phi^2\right)^2 + \lambda_3^2 v_h^2 v_\phi^2}\Bigg] \\
= \tan^{-1}\Bigg[&\frac{1}{\lambda_3\sqrt{\lambda_3\mu_\phi^2 - 2\mu_h^2\lambda_\phi}\sqrt{\lambda_3\mu_h^2 - 2\lambda_h\mu_\phi^2}}\Bigg(\lambda_h(2\lambda_\phi + \lambda_3)\mu_\phi^2 - (2\lambda_h + \lambda_3)\mu_h^2\lambda_\phi \\
&+ \sqrt{\lambda_3^2(\lambda_3\mu_\phi^2 - 2\mu_h^2\lambda_\phi)(\lambda_3\mu_h^2 - 2\lambda_h\mu_\phi^2) + ((2\lambda_h + \lambda_3)\mu_h^2\lambda_\phi - \lambda_h(2\lambda_\phi + \lambda_3)\mu_\phi^2)^2)}\Bigg)\Bigg]
\end{aligned}
$$

Appendix B: $V(h', \phi')$

$$
\begin{aligned}
V(h',\phi') = &\frac{1}{4}\lambda_h \left(h'\right)^4 \cos^4\theta + \frac{1}{4}\lambda_\phi \left(\phi'\right)^4 \cos^4\theta + \frac{1}{4}\lambda_3 \left(h'\right)^2 \left(\phi'\right)^2 \cos^4\theta \\
&+ v_h\lambda_h \left(h'\right)^3 \cos^3\theta + v_\phi\lambda_\phi \left(\phi'\right)^3 \cos^3\theta - \frac{1}{2}\sin\theta\lambda_3 h' \left(\phi'\right)^3 \cos^3\theta \\
&+ \sin\theta\lambda_\phi h' \left(\phi'\right)^3 \cos^3\theta + \frac{1}{2}v_h\lambda_3 h' \left(\phi'\right)^2 \cos^3\theta + \frac{1}{2}\sin\theta\lambda_3 \left(h'\right)^3 \phi' \cos^3\theta \\
&- \sin\theta\lambda_h \left(h'\right)^3 \phi' \cos^3\theta + \frac{1}{2}v_\phi\lambda_3 \left(h'\right)^2 \phi' \cos^3\theta + \frac{1}{4}\sin^2\theta\lambda_3 \left(h'\right)^4 \cos^2\theta \\
&+ \frac{1}{4}\sin^2\theta\lambda_3 \left(\phi'\right)^4 \cos^2\theta + \frac{1}{2}\sin\theta v_\phi\lambda_3 \left(h'\right)^3 \cos^2\theta - \frac{1}{2}\sin\theta v_h\lambda_3 \left(\phi'\right)^3 \cos^2\theta \\
&- \frac{1}{2}\mu_h^2 \left(h'\right)^2 \cos^2\theta + \frac{1}{4}v_\phi^2\lambda_3 \left(h'\right)^2 \cos^2\theta + \frac{3}{2}v_h^2\lambda_h \left(h'\right)^2 \cos^2\theta - \frac{1}{2}\mu_\phi^2 \left(\phi'\right)^2 \cos^2\theta \\
&- \sin^2\theta\lambda_3 \left(h'\right)^2 \left(\phi'\right)^2 \cos^2\theta + \frac{3}{2}\sin^2\theta\lambda_h \left(h'\right)^2 \left(\phi'\right)^2 \cos^2\theta \\
&+ \frac{3}{2}\sin^2\theta\lambda_\phi \left(h'\right)^2 \left(\phi'\right)^2 \cos^2\theta + \frac{1}{4}v_h^2\lambda_3 \left(\phi'\right)^2 \cos^2\theta + \frac{3}{2}v_\phi^2\lambda_\phi \left(\phi'\right)^2 \cos^2\theta \\
&- \sin\theta v_\phi\lambda_3 h' \left(\phi'\right)^2 \cos^2\theta + 3\sin\theta v_\phi\lambda_\phi h' \left(\phi'\right)^2 \cos^2\theta + \sin\theta v_h\lambda_3 \left(h'\right)^2 \phi' \cos^2\theta \\
&- 3\sin\theta v_h\lambda_h \left(h'\right)^2 \phi' \cos^2\theta + v_h v_\phi\lambda_3 h'\phi' \cos^2\theta + \frac{1}{2}\sin^2\theta v_h\lambda_3 \left(h'\right)^3 \cos\theta \\
&+ \frac{1}{2}\sin^2\theta v_\phi\lambda_3 \left(\phi'\right)^3 \cos\theta + \frac{1}{2}\sin^3\theta\lambda_3 h' \left(\phi'\right)^3 \cos\theta - \sin^3\theta\lambda_h h' \left(\phi'\right)^3 \cos\theta \\
&+ \sin\theta v_h v_\phi\lambda_3 \left(h'\right)^2 \cos\theta - \sin\theta v_h v_\phi\lambda_3 \left(\phi'\right)^2 \cos\theta - \sin^2\theta v_h\lambda_3 h' \left(\phi'\right)^2 \cos\theta \\
&+ 3\sin^2\theta v_h\lambda_h h' \left(\phi'\right)^2 \cos\theta - v_h\mu_h^2 h' \cos\theta + \frac{1}{2}v_h v_{\phi\phi}^2\lambda_3 h' \cos\theta + v_h^3\lambda_h h' \cos\theta \\
&- \frac{1}{2}\sin^3\theta\lambda_3 \left(h'\right)^3 \phi' \cos\theta + \sin^3\theta\lambda_\phi \left(h'\right)^3 \phi' \cos\theta - v_\phi\mu_\phi^2\phi' \cos\theta \\
&- \sin^2\theta v_\phi\lambda_3 \left(h'\right)^2 \phi' \cos\theta + 3\sin^2\theta v_\phi\lambda_\phi \left(h'\right)^2 \phi' \cos\theta + \frac{1}{2}v_h^2 v_\phi\lambda_3\phi' \cos\theta \\
&+ v_{\phi\phi}^3\lambda_\phi\phi' \cos\theta + \sin\theta\mu_h^2 h'\phi' \cos\theta - \sin\theta\mu_\phi^2 h'\phi' \cos\theta + \frac{1}{2}\sin\theta v_h^2\lambda_3 h'\phi' \cos\theta + \ldots
\end{aligned}
$$

$$
\begin{aligned}
...&-\frac{1}{2}\sin\theta v_\phi^2\lambda_3 h'\phi'\cos\theta-3\sin\theta v_h^2\lambda_h h'\phi'\cos\theta+3\sin\theta v_\phi^2\lambda_\phi h'\phi'\cos\theta\\
&+\frac{1}{4}\sin^4\theta\lambda_\phi\left(h'\right)^4+\frac{1}{4}\sin^4\theta\lambda_h\left(\phi'\right)^4+\sin^3\theta v_\phi\lambda_{\phi\phi}\left(h'\right)^3-\sin^3\theta v_h\lambda_h\left(\phi'\right)^3\\
&-\frac{1}{2}v_h^2\mu_h^2-\frac{1}{2}v_\phi^2\mu_\phi^2-\frac{1}{2}\sin^2\theta\mu_\phi^2\left(h'\right)^2+\frac{1}{4}\sin^2\theta v_h^2\lambda_3\left(h'\right)^2+\frac{3}{2}\sin^2\theta v_\phi^2\lambda_\phi\left(h'\right)^2\\
&-\frac{1}{2}\sin^2\theta\mu_h^2\left(\phi'\right)^2+\frac{1}{4}\sin^4\theta\lambda_3\left(h'\right)^2\left(\phi'\right)^2+\frac{1}{4}\sin^2\theta v_\phi^2\lambda_3\left(\phi'\right)^2+\frac{3}{2}\sin^2\theta v_h^2\lambda_h\left(\phi'\right)^2\\
&+\frac{1}{2}\sin^3\theta v_\phi\lambda_3 h'\left(\phi'\right)^2+\frac{1}{4}v_h^2v_\phi^2\lambda_3+\frac{1}{4}v_h^4\lambda_h+\frac{1}{4}v_\phi^4\lambda_\phi-\sin\theta v_\phi\mu_\phi^2h'+\frac{1}{2}\sin\theta v_h^2v_\phi\lambda_3h'\\
&+\sin\theta v_\phi^3\lambda_\phi h'+\sin\theta v_h\mu_h^2\phi'-\frac{1}{2}\sin^3\theta v_h\lambda_3\left(h'\right)^2\phi'-\frac{1}{2}\sin\theta v_h v_\phi^2\lambda_3\phi'-\sin\theta v_h^3\lambda_h\phi'\\
&-\sin^2\theta v_h v_\phi\lambda_3 h'\phi'
\end{aligned}
$$

Appendix C: Feynman rules

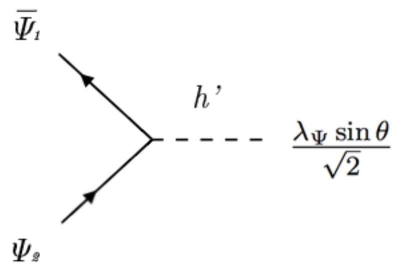

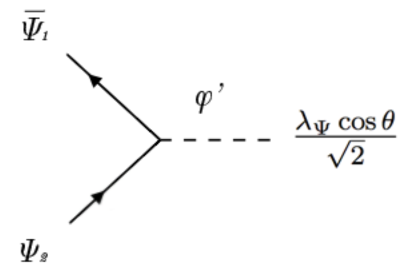

Figure 8: Vertex factors between $\bar{\Psi}_1$ and Ψ_2 and the scalars h' and ϕ'.

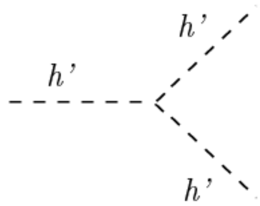

$$A_{hhh} = v_h \cos\theta \left[\sin^2\theta\lambda_3 + 2\cos^2\theta\lambda_h\right] + v_\phi \sin\theta \left[\cos^2\theta\lambda_3 + 2\sin^2\theta\lambda_\phi\right]$$

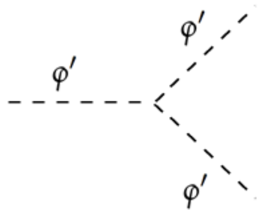

$$A_{\phi\phi\phi} = v_\phi \cos\theta \left[\sin^2\theta\lambda_3 + 2\cos^2\theta\lambda_\phi\right] + v_h \sin\theta \left[\cos^2\theta\lambda_3 + 2\sin^2\theta\lambda_h\right]$$

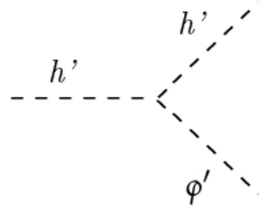

$$A_{hh\phi} = \frac{1}{4} v_\phi \cos\theta \left[(-1 + 3\cos 2\theta)\lambda_3 + 12\sin^2\theta\lambda_\phi\right] - \frac{1}{4} v_h \sin\theta \left[(1 + 3\cos 2\theta)\lambda_3 - 12\sin^2\theta\lambda_h\right]$$

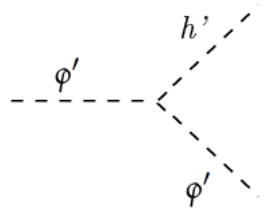

$$A_{h\phi\phi} = \frac{1}{4} v_h \cos\theta \left[(-1 + 3\cos 2\theta)\lambda_3 + 12\sin^2\theta\lambda_h\right] - \frac{1}{4} v_\phi \sin\theta \left[(1 + 3\cos 2\theta)\lambda_3 - 12\sin^2\theta\lambda_\phi\right]$$

Figure 9: Vertex factors between the scalars h' and ϕ'.